



FACULDADE DE MEDICINA DA UNIVERSIDADE DE COIMBRA

MESTRADO INTEGRADO EM MEDICINA – TRABALHO FINAL

ANA TERESA ANTUNES SIMÕES

***Identification of the toxic fragment of ataxin-3 protein in  
Machado-Joseph disease***

ARTIGO CIENTÍFICO

ÁREA CIENTÍFICA DE NEUROLOGIA

Trabalho realizado sob a orientação de:

LUÍS PEREIRA DE ALMEIDA

MARIA CRISTINA JANUÁRIO SANTOS

MARÇO/2018

# Identification of the toxic fragment of ataxin-3 protein in Machado-Joseph disease

Ana Teresa Antunes Simões

MARÇO 2018



UNIVERSIDADE DE COIMBRA

# Identification of the toxic fragment of ataxin-3 protein in Machado-Joseph disease

Ana Teresa Antunes Simões

Thesis submitted to the Faculty of Medicine of the University of Coimbra for the attribution of the Master degree in Medicine.

Tese apresentada à Faculdade de Medicina da Universidade de Coimbra para prestação de provas de mestrado em Medicina.

MARÇO 2018



UNIVERSIDADE DE COIMBRA

# Identification of the toxic fragment of ataxin-3 protein in Machado-Joseph disease

The research work presented in this thesis was performed at the Center for Neuroscience and Cell Biology of Coimbra, Portugal, under supervision of Luís Pereira de Almeida, PhD and Maria Cristina Januário Santos, PhD.

O trabalho experimental apresentado nesta tese foi elaborado no Centro de Neurociências e Biologia Celular de Coimbra, Portugal, sob supervisão do Professor Doutor Luís Pereira de Almeida e Professora Doutora Maria Cristina Januário Santos.

This work was funded by the ERDF through the Regional Operational Program Center 2020, Competitiveness Factors Operational Program (COMPETE 2020) and National Funds through FCT (Foundation for Science and Technology) - BrainHealth2020 projects (CENTRO-01-0145-FEDER-000008), ViraVector (CENTRO-01-0145-FEDER-022095), CortaCAGs (POCI-01-0145-FEDER-016719) and POCI-01-0145-FEDER-007440, as well as SFRH/BPD/87341/2012, SFRH/BD/87048/2012, SFRH/BD/74993/2010 and SFRH/BD/87404/2012 to ATS, VC, JDN and JCS, respectively (FCT), and AFM-Telethon and the SynSpread, ESMI and ModelPolyQ under the EU Joint Program - Neurodegenerative Disease Research (JPND), the last two co-funded by the European Union H2020 program, GA No.643417; by National Ataxia Foundation (USA), the American Portuguese Biomedical Research Fund (APBRF) and the Richard Chin and Lily Lock Machado-Joseph Disease Research Fund.

Este trabalho foi financiado pelo FEDER através do Programa Operacional Regional Centro 2020, do Programa Operacional de Fatores de Competitividade (COMPETE 2020) e por Fundos Nacionais através da FCT (Fundação para a Ciência e a Tecnologia) – projetos BrainHealth2020 (CENTRO-01-0145-FEDER-000008), ViraVector (CENTRO-01-0145-FEDER- 022095), CortaCAGs (POCI-01-0145-FEDER-016719) e POCI-01-0145-FEDER-007440, bem como SFRH/BPD/87341/2012, SFRH/BD/87048/2012, SFRH/BD/74993/2010 e SFRH/BD/87404/2012 a ATS, VC, JDN e JCS, respetivamente, e pelos SynSpread, ESMI e ModelPolyQ no âmbito do EU Joint Programme - Neurodegenerative Disease Research (JPND), os dois últimos co-financiados pelo programa H2020 da União Europeia, GA No. 643417; ainda pela “National Ataxia Foundation” (USA), pelo American Portuguese Biomedical Research Fund (APBRF) e pelo Richard Chin and Lily Lock Machado Joseph Disease Research Fund.



**FCT** Fundação para a Ciência e a Tecnologia  
MINISTÉRIO DA CIÊNCIA E DO ENSINO SUPERIOR

Portugal



Part of this work was presented as an oral communication at Ataxia Research Conference 2015, Old Windsor, England; March 25-28, 2015;



and at the XLVII Annual Meeting of the Portuguese Pharmacological Society, Coimbra, Portugal; February 2-4, 2017.



## References

Simões AT, Carmona V, Duarte-Neves J, Cunha-Santos J, Pereira de Almeida L; "*Identification of the calpain cleavage sites in ataxin-3 protein*"; Ataxia Research Conference 2015, Old Windsor, England; March 25-28, 2015

Simões AT, Carmona V, Duarte-Neves J, Cunha-Santos J, Pereira de Almeida L; "*Identification of the calpain cleavage sites in ataxin-3 protein*"; XLVII Annual Meeting of the Portuguese Pharmacological Society, Coimbra, Portugal; February 2-4, 2017

*Ao meu marido e filhos*

*Nélio, Leonardo e Lourenço*

## **Acknowledgements/ Agradecimentos**

Ao Professor Doutor Luís Pereira de Almeida agradeço a sua orientação científica, apoio e incentivo no decurso de mais uma tese. Agradeço ainda a sua confiança depositada em mim e amizade que sempre demonstrou.

À Professora Doutora Maria Cristina Januário agradeço a sua orientação científica e apoio durante este trabalho.

Agradeço a todos os meus colegas e amigos do Centro de Neurociências e Biologia Celular de Coimbra, em especial a Vítor Carmona, pela amizade e por ter sido o meu braço direito neste trabalho, e a Joana Neves e Janete Santos pela amizade, boa disposição e por terem sido também fundamentais na execução deste trabalho.

Aos meus amigos da vida e aos novos da faculdade, em especial à Filipa, Vera, Leandro, Sandra, Carina, Fátima, Raquel, Rita, João, Joana e Guilherme, agradeço a sua amizade e as palavras de encorajamento.

Um agradecimento muito especial ao Nélio Gonçalves, meu marido. Agradeço pelo apoio, dedicação, discussão científica, encorajamento, amizade, paciência e carinho essenciais para que depois de uma caminhada me desse alento a iniciar outra, que não teria concluído sem a sua ajuda incondicional, comigo e com os nossos filhos.

Dois agradecimentos particulares aos meus filhos Leonardo e Lourenço, que durante a gravidez também foram a aulas, orais e exames e me ajudaram diariamente a suavizar os dias e a relativizar sempre as dificuldades. A eles lhes dedico esta tese e por eles ambiciono um futuro melhor.

Finalmente, um agradecimento profundo à minha família, em especial aos meus pais Jorge e Lurdes, aos meus sogros Ernesto e Ilídia, aos meus irmãos Francisco e Ricardo, aos meus cunhados e cunhadas Daniel, Vítor, Liliana, Amélia, Margarida e Cândida, e aos meus sobrinhos Francisca, Mariana, Duarte e António. Agradeço por acreditarem em mim e por me darem muita força.

Esta tese é-vos dedicada.

## TABLE OF CONTENTS

<b>Abbreviations .....</b>	<b>2</b>
<b>Affiliation .....</b>	<b>3</b>
<b>Abstract .....</b>	<b>4</b>
<b>Resumo .....</b>	<b>6</b>
<b>Introduction .....</b>	<b>8</b>
<b>Materials and methods .....</b>	<b>11</b>
<b>Results .....</b>	<b>18</b>
<b>Discussion and conclusions .....</b>	<b>35</b>
<b>Acknowledgements .....</b>	<b>40</b>
<b>Funding .....</b>	<b>40</b>
<b>References .....</b>	<b>41</b>



## ABBREVIATIONS

ATX-3	Ataxin-3
BSA	Bovine serum albumin
CAG	Cytosine-adenine-guanine
DAPI	4',6-diamino-2-phenylindole
DARPP-32	Dopamine- and cyclic AMP-regulated phosphoprotein of 32 kDa
DNA	Deoxyribonucleic acid
HEK	Human embryonic kidney cell line
iPSC	Induced pluripotent stem cell
MJD	Machado-Joseph disease
NES	Nuclear export signal
NLS	Nuclear localization signal
PBS	Phosphate-buffered saline
PFA	Paraphormaldehyde
PGK	Phosphoglycerate kinase 1
polyQ	Polyglutamine
PCR	Polymerase chain reaction
RT	Room temperature
SCA	Spinocerebellar ataxia
UIM	Ubiquitin interacting motif

## Identification of the toxic fragment of ataxin-3 protein in Machado-Joseph disease

Ana Teresa Simões<sup>1,2</sup>, Vítor Carmona<sup>2</sup>, Joana Duarte-Neves<sup>2</sup>, Janete Cunha-Santos<sup>2</sup>, Cristina Januário<sup>1,3</sup>, Luís Pereira de Almeida<sup>2,4,\*</sup>

<sup>1</sup>Faculty of Medicine, University of Coimbra, Coimbra 3000-354, Portugal

<sup>2</sup>CNC – Center for Neuroscience and Cell Biology, Coimbra 3004-504, Portugal

<sup>3</sup>Coimbra Hospital and University Centre, Neurology Department, Coimbra 3000-075, Portugal

<sup>4</sup>Faculty of Pharmacy, University of Coimbra, Coimbra 3000-354, Portugal

\*To whom correspondence should be addressed at: CNC – Center for Neuroscience and Cell Biology, University of Coimbra, Rua Larga, Coimbra 3004-504, Portugal, Tel: +351 966337482; Fax: +351 239853409; Email: [luispa@cnc.uc.pt](mailto:luispa@cnc.uc.pt)

## ABSTRACT

Machado-Joseph disease (MJD) is the most frequent dominantly-inherited cerebellar ataxia worldwide. Over-repetition of a CAG trinucleotide in the *MJD1* gene translates into a polyglutamine tract within the ataxin-3 protein, which upon proteolysis may trigger MJD. Calpains are calcium-dependent cysteine proteases, which mediate the formation of toxic fragments, ataxin-3 translocation to the nucleus and neurodegeneration.

The aim of this project was to understand *in vivo* the calpains contribution to MJD pathogenesis. In particular, we investigated a) the calpain cleavage sites in ataxin-3 protein *in vivo*, b) which generated calpain cleavage fragment is more toxic and more drastically contributing to ataxin-3 nuclear localization, aggregation and neurotoxicity, c) whether calpain cleavage sites deletion can prevent morphologic alterations and be envisioned as a therapeutic strategy for MJD, and d) the importance of the nuclear localization signal (NLS) sequence to pathology.

For this, we generated calpain-resistant constructs and truncated forms at the predicted cleavage sites of ataxin-3 by inverse PCR mutagenesis. These constructs were then expressed by lentiviral vectors transduction of the adult mouse brain. We identified the putative calpain cleavage sites for both wild-type and mutant ataxin-3. Western-blot analysis confirmed that the mutation of these sites led to the abrogation of the toxic fragments formation. Furthermore, immunohistochemical analysis using an anti-DARPP-32 antibody suggested that the 26 kDa fragment is the major contributor for striatal degeneration, independently of the NLS sequence, further confirmed by cresyl violet staining. Nevertheless, simultaneous decrease of the 26 and 34 kDa fragments formation is required for modification of subcellular localization of ataxin-3 from aggregated intranuclear into diffuse cytoplasmic localization within neurons. A neuroprotective effect is observed upon calpain cleavage sites mutagenesis.

In conclusion, these results support the idea that ataxin-3 cleavage by calpains is required for the subsequent aggregation process and that the simple mutation of calpain cleavage sites can reduce mutant ataxin-3 aggregation by suppressing its proteolysis. Therefore, these findings suggest that the calpain system should be considered for MJD therapeutic intervention and also for other neurodegenerative diseases vulnerable to calcium deregulation. Furthermore, the identification of the calpain cleavage sites will allow the design of specific drugs or the use of tools for genome editing at a specific location.

## **KEYWORDS**

Machado-Joseph disease, calpains, proteolysis, ataxin-3, toxic fragment

## RESUMO

A doença de Machado-Joseph (DMJ) é a ataxia cerebelosa autossômica dominante mais comum a nível mundial. A repetição do trinucleotídeo CAG no gene *MJD1* é traduzida numa cadeia de poliglutaminas na proteína ataxina-3. Há evidências que a proteólise desta proteína está envolvida no despoletar da DMJ. As calpaínas são cisteína-proteases dependentes de cálcio e medeiam a formação de fragmentos tóxicos, a translocação da ataxina-3 para o núcleo e neurodegenerescência.

O objetivo deste projeto foi compreender *in vivo* a contribuição das calpaínas na patogénese da DMJ. Em particular, investigámos a) os locais de clivagem pelas calpaínas da proteína ataxina-3, b) qual o fragmento gerado pela clivagem mais tóxico e que mais drasticamente contribui para a localização nuclear da ataxina-3, agregação e neurotoxicidade, c) se a deleção dos locais de clivagem pelas calpaínas poderia prevenir alterações morfológicas e se poderia ser considerada como uma estratégia terapêutica para a DMJ, e d) a importância do sinal de localização nuclear (NLS) para a patologia.

Para tal, gerámos construções resistentes às calpaínas e as formas truncadas nos locais previstos de clivagem da ataxina-3 por mutagénese por PCR invertido. Estas construções foram depois expressas por transdução de vetores lentivirais no cérebro de murganho adulto. Identificámos os presumíveis locais de clivagem pelas calpaínas tanto da ataxina-3 nativa como da mutante. A análise por Western-blot confirmou que a mutação destes locais conduziu à diminuição da formação dos fragmentos tóxicos. Adicionalmente, a análise imunohistoquímica usando o anticorpo anti-DARPP-32 sugeriu que é o fragmento de 26 kDa aquele que mais contribui para a degenerescência estriatal, independentemente da sequência NLS, confirmação esta reforçada por análise de secções submetidas a coloração de violeta de cresilo. No entanto, é necessária a diminuição simultânea da formação dos fragmentos de 26 e 34 kDa para que haja

modificação da localização subcelular da ataxina-3 de agregados intranucleares para localização citoplasmática difusa nos neurónios. A mutagénesse dos locais de clivagem pelas calpaínas promove um efeito neuroprotetor.

Em resumo, estes resultados suportam a hipótese de que a clivagem da ataxina-3 pelas calpaínas é necessária ao subsequente processo de agregação e que a simples mutação dos locais de clivagem pelas calpaínas pode reduzir a agregação da ataxina-3 mutante por supressão da sua proteólise. Sendo assim, este trabalho sugere que o sistema de calpaínas deverá ser considerado como alvo de intervenção terapêutica na DMJ e em outras doenças neurodegenerativas vulneráveis à desregulação de cálcio. Acresce que a identificação dos locais de clivagem pelas calpaínas permitirá o desenvolvimento de fármacos mais específicos ou o uso de tecnologias de edição génica num local determinado.

## **PALAVRAS-CHAVE**

Doença de Machado-Joseph, calpaínas, proteólise, ataxina-3, fragmento tóxico

## INTRODUCTION

Machado-Joseph disease, also known as spinocerebellar ataxia type 3 (MJD/SCA3), is the most frequent autosomal dominantly-inherited ataxia worldwide, originally described in emigrants in Northern American families from the Portuguese Azorean islands São Miguel (Machado family) and Flores (Joseph family) (1). MJD is caused by a CAG expansion within the coding region of *MJD1* gene mapped to chromosome 14q32.1, resulting the mutation in an abnormal polyglutamine tract at the C-terminal of ataxin-3, a protein implicated in cellular quality control (2).

According to the toxic fragment hypothesis, neurotoxicity might derive from the proteolysis of the host protein to liberate a polyglutamine fragment, an event suggested to be the trigger of the aggregation process, a hallmark of the disease (3). Furthermore, an ataxin-3 fragment was detected in Q71 transgenic mice and *post mortem* brain tissue of MJD patients, whose levels increased with disease severity, supporting a relation between ataxin-3 cleavage and disease progression (4). Accordingly, Ikeda and collaborators (1996) who developed the first transgenic mouse model of MJD found no pathology upon expression of full-length ataxin-3, while truncated protein produced a strong phenotype (5). Therefore, identifying protease(s) responsible for human mutant ataxin-3 processing and its cleavage site(s) could contribute to understand the mechanism of proteolysis involved and reveal potential candidates for therapy. In this sense, mutant ataxin-3 has been shown to be a substrate for caspases (6-8) and calpains (9-14), though without consensual results.

Ataxin-3 is present both in cytoplasm and nucleus, being the nucleus considered an important subcellular localization for polyglutamine pathogenesis (15). In fact, Bichelmeier and collaborators (2007) demonstrated in MJD transgenic mice that nuclear localization of ataxin-3 is required for the manifestation of symptoms (16). Ataxin-3 nucleocytoplasmic shuttling

activity was shown to be promoted by a) recognition of specific nuclear localization signals (NLS) or nuclear export signals (NES) (17), b) phosphorylation on serine residues within ataxin-3 (18), c) proteotoxic stress, such as heat shock and oxidative stress (19), and d) calpain-mediated proteolysis, the ataxin-3 fragments being able to cross the nuclear pore and accumulate in the nucleus (12). Numerous downstream effects including accumulation and apoptotic activation, misfolding, aggregation, and sequestration of other proteins including transcription factors and chaperones may then be initiated leading ultimately to neurodegeneration.

Our previous findings demonstrated for the first time *in vivo*, without external protease activation, that calpain-mediated proteolysis has a determinant role not only in ataxin-3 toxic fragments formation, but also in ataxin-3 translocation to the nucleus and MJD pathogenesis (12). Nevertheless, the exact sites for calpain cleavage had never been addressed until recently, in a study developed in HEK 293T cells with calpain activity triggered by ionomycin and  $\text{CaCl}_2$  (14). However, the identification of the exact sites without external protease activation and *in vivo*, the differential cleavage between wild-type and mutant ataxin-3, the impact of the resulting different fragments to aggregation, which fragment is more toxic and if the simple deletion of the calpain cleavage sites is neuroprotective remained elusive. In this work, results show that the calpain cleavage site for wild-type ataxin-3 is the amino acid 194, while for the mutant ataxin-3 are the amino acids 253 and 273. Although the major contributor for striatal degeneration is the 26 kDa fragment, independently of the presence of the NLS, the decrease of both 26 and 34 kDa fragments formation is required for mutant ataxin-3 to locate diffusely in the cytoplasm. Calpain-resistant constructs reduce loss of DARPP-32 immunoreactivity suggesting a neuroprotective effect.

Overall, these results suggest that the calpain-mediated proteolysis should be used for the development of viable therapeutic interventions. Delineating the role of calpains in MJD



will also lead to greater understanding of the core mechanisms of neuronal death in other neurodegenerative disorders.

## **MATERIALS AND METHODS**

### **Vectors construction**

Delta ( $\Delta$ ) and truncated (T) ataxin-3 vectors were constructed using inverted PCR mutagenesis. Briefly, two phosphorylated oligonucleotides (Eurofins) were designed in order to amplify the parental vectors full sequence (LTR-SIN-PGK-Atxn3-72Q-LTR or LTR-SIN-PGK-Atxn3-27Q-LTR (20)) with the exception of: 1) the sequence corresponding to the five amino acids to be deleted, in the case of  $\Delta$  constructs; full length ataxin-3 bearing  $\Delta$ 194: deletion of the sequence 192-196;  $\Delta$ 253: deletion of the sequence 251-255;  $\Delta$ 273: deletion of the sequence 271-275 and  $\Delta$ 282: deletion of the sequence 280-284; 2) the sequence corresponding to the amino acids of the N-terminal part of the protein, until the C-end of the aforementioned selected interval of five amino acids, in the case of truncated constructs; C-terminal ataxin-3 fragment starting at position 197 (T197); 256 (T256); 276 (T276) and 285 (T285). Mutagenesis was performed using Phusion High-Fidelity DNA polymerase (Thermo Scientific) and a standard protocol for GC rich templates. Linear products were circularized using T4 DNA ligase (Life technologies) and transformed into TOP10 chemically competent cells (Life technologies) according to the manufacturer's instructions. All constructs were verified by restriction analysis and sequencing.

### **Cell culture**

HEK 293T cells were maintained in standard DMEM (Sigma) supplemented with 10% fetal bovine serum (Life Technologies) and 1% Penicillin/Streptomycin (Life Technologies) in a humid incubator (5% CO<sub>2</sub>/ 95% air at 37°C).

For the transfection of HEK 293T,  $2,75 \times 10^5$  cells were plated per well on 12-well tissue treated plates. After 24 hours, transfection was performed by replacing the culture medium with a mixture of DNA/polyethylenimine complexes containing 750 ng of plasmid DNA. Cell collection for western blotting was performed 48 hours post-transfection.

### **Viral vectors production**

Lentiviral vectors encoding human wild-type ataxin-3 (ATX-3 27Q), mutant ataxin-3 (ATX-3 72Q) (20) and the respective truncated (27Q T197, 72Q T256, 72Q T276 and 72Q T285) and calpain-resistant (27Q  $\Delta$ 194, 72Q  $\Delta$ 253, 72Q  $\Delta$ 273 and 72Q  $\Delta$ 282) forms were produced in 293T cells with a four-plasmid system, as previously described (21). The lentiviral particles were resuspended in 1% bovine serum albumin (BSA) in phosphate-buffered saline (PBS). The viral particle content of batches was determined by quantitative PCR (qPCR) using primers for WPRE for detection and albumin for normalization of the amount of genomic DNA, as described in (22). Viral stocks were stored at  $-80^\circ\text{C}$  until use.

### **Animals**

4-week-old C57BL/6J mice (Charles River) were used for the lentiviral vectors injection in the striatum.

The animals were housed in a temperature-controlled room maintained on a 12 h light / 12 h dark cycle. Food and water were provided ad libitum. The experiments were carried out in accordance with the European Union Directive 2010/63/EU covering the protection of animals used for scientific purposes. The researchers received adequate training (FELASA-

certified course) and certification to perform the experiments from the Portuguese authorities (Direção Geral de Alimentação e Veterinária).

### ***In vivo* injection in the striatum**

Concentrated viral stocks were thawed on ice. Lentiviral vectors encoding human wild-type (ATX-3 27Q) or mutant ataxin-3 (ATX-3 72Q) and the respective truncated (ATX-3 T<sub>N-term</sub>, 27Q T197, 72Q T256, 72Q T276 and 72Q T285) or calpain-resistant (27Q  $\Delta$ 194, 72Q  $\Delta$ 253, 72Q  $\Delta$ 273 and 72Q  $\Delta$ 282) forms were stereotaxically injected into the striatum in the following coordinates: anteroposterior: +0.6mm; medial-lateral:  $\pm$ 1.8mm; dorsoventral: -3.3mm. Animals were anesthetized by administration of avertin (200  $\mu$ g/g, intraperitoneally).

For western-blot procedure, wild-type mice received a single 2  $\mu$ l injection of 0.3 mg of p24/ml lentivirus in each side: left hemisphere (ATX-3 27Q) and right hemisphere (ATX-3 72Q) or left hemisphere (truncated form) and right hemisphere (calpain-resistant form). For immunohistochemical procedure, wild-type mice received a single 1  $\mu$ l injection of 0.4 mg of p24/ml lentivirus in each side: left hemisphere (ATX-3 27Q) and right hemisphere (ATX-3 72Q) or left hemisphere (truncated form) and right hemisphere (calpain-resistant form). Mice were kept in their home cages for 5 and 8 weeks, before being sacrificed for immunohistochemical and western-blot analysis.

### **Immunohistochemical procedure**

After an overdose of avertin (2.5x 200  $\mu$ g/g, i.p.), transcardial perfusion of the mice was performed with a phosphate solution followed by fixation with 4% paraformaldehyde (PFA). The brains were removed and post-fixed in 4% PFA for 24h and cryoprotected by incubation

in 25% sucrose/ phosphate buffer for 48 h. The brains were frozen, 25 µm coronal striatal sections were cut using a cryostat (LEICA CM3050 S) at -21°C. Slices throughout the entire brain regions were collected in anatomical series and stored in 48-well trays as free-floating sections in PBS supplemented with 0.05 µM sodium azide. The trays were stored at 4°C until immunohistochemical processing.

Sections from injected mice were processed with the following primary antibodies: a mouse monoclonal anti-ataxin-3 antibody (1H9, 1:5000; Chemicon, Temecula, CA), recognizing the human ataxin-3 fragment from amino acids F112-L249; a mouse monoclonal anti-myc tag antibody (clone 4A6, 1:1000; Cell Signaling); a rabbit anti-DARPP-32 antibody (1:1000; Chemicon, Temecula, CA), followed by incubation with the respective biotinylated secondary antibodies (1:200; Vector Laboratories). Bound antibodies were visualized using the Vectastain ABC kit, with 3,3'-diaminobenzidine tetrahydrochloride (DAB metal concentrate; Pierce) as substrate. Dry sections were mounted in gelatin-coated slides, dehydrated with ethanol solutions and Xylene Substitute (Sigma-Aldrich), and mounted in Eukitt quick-hardening mounting medium (Sigma-Aldrich).

Double stainings for the N-terminal of ataxin-3 (clone 4A6, 1:1000; Cell Signaling), nuclear marker (DAPI, blue, 1:5000, Sigma) and ubiquitin (Dako, 1:1000; Cambridgeshire, UK) were performed.

Free-floating sections from injected mice were at RT for 2 h in PBS/0.1% Triton X-100 containing 10% NGS (Gibco), and then overnight at 4°C in blocking solution with the primary antibodies. Sections were washed three times and incubated for 2 h at RT with the corresponding secondary antibodies coupled to fluorophores (1:200; Molecular Probes, Oregon, USA) diluted in the respective blocking solution. The sections were washed three times and then mounted in mowiol (Sigma) on microscope slides.

Staining was visualized using Zeiss Axioskop 2 plus, Zeiss Axiovert 200 and Zeiss LSM 510 Meta imaging microscopes (Carl Zeiss Microimaging, Germany), equipped with AxioCam HR color digital cameras (Carl Zeiss Microimaging) using 5x, 20x, 40x and 63x Plan-Neofluar and a 63x Plan/Apochromat objectives and the AxioVision 4.8 and Zeiss LSM510 software packages (Carl Zeiss Microimaging).

### **Cresyl violet staining**

Coronal 25- $\mu$ m-thick striatal sections were cut using a cryostat. Premounted sections were stained with cresyl violet for 30 secs, differentiated in 70% ethanol, dehydrated by passing twice through 95% ethanol, 100% ethanol and xylene solutions, and mounted onto gelatin-coated microscope slides with Eukitt<sup>®</sup> (Sigma).

### **Evaluation of the volume of the DARPP-32 depleted volume**

The extent of ataxin-3 lesions in the striatum was analyzed by photographing, with a 1.25x objective, ten DARPP-32 stained sections per animal (at 200  $\mu$ m intervals), selected so as to obtain complete sampling of the striatum, and by quantifying the area of the lesion with a semiautomated image-analysis software package (Image J software, USA). The volume was then estimated with the following formula:  $\text{volume} = d(a_1+a_2+a_3 \dots)$ , where  $d$  is the distance between serial sections and  $a_1+a_2+a_3$  are the areas for individual serial sections.

## **Cell counts and morphometric analysis of ataxin-3 inclusions**

Ten coronal sections per animal, that were distanced 200  $\mu\text{m}$  from each other, showing complete rostrocaudal sampling of the striatum were scanned with a 20x objective. The analyzed areas of the striatum encompassed the entire region containing ATX-3 inclusions, as revealed by staining with the anti-ataxin-3 antibodies. Total number of inclusions were manually counted in all ten sections and multiplied by eight to account for the intermediate sections using a semiautomated image-analysis software package (Image J software, USA).

Ataxin-3 nuclear localization was assessed by scanning the area above the needle tract in three different sections per animal, using a 63x objective. Quantification analysis was performed by multiplying the number of observed inclusions per one attributable value of subcellular localization, considering value 1 for nuclear localization, 0.5 for both nuclear and cytoplasmic localization and 0.001 for cytoplasmic localization.

## **Western-blot analysis**

Monolayer cells were scraped in radioimmunoprecipitation lysis buffer (50 mM Tris-HCl, pH 8, 150 mM NaCl, 1% NP-40, 0.5% sodium deoxycholate and 0.1% sodium dodecyl sulfate) containing protease inhibitors (Roche) followed by sonication by two series of 4 s pulses.

For assessment of ataxin-3 proteolysis and aggregation in the lentiviral model of MJD, transcardial perfusion of the mice was performed with ice-cold phosphate buffered saline containing 10 mM EDTA and 10 mM of the alkylating reagent N-ethylmaleimide, to avoid post-mortem calpain overactivation. The injected striata were then dissected and immediately

sonicated in RIPA buffer (50 mM Tris-HCl, pH 7.4, 150 mM NaCl, 7 mM EDTA, 1% NP-40, 0.1% SDS, 10 µg/ml DTT, 1mM PMSF, 200 µg/ml leupeptin, protease inhibitors cocktail).

Equal amounts (20 µg of protein) were resolved on 12% SDS-polyacrylamide gels and transferred onto PVDF membranes. Immunoblotting was performed using the monoclonal anti-ataxin-3 antibody (1H9, 1:1000; Chemicon, Temecula, CA), monoclonal anti-myc tag (clone 4A6, 1:1000; Cell Signaling) and monoclonal anti-β-actin (clone AC-74, 1:5000; Sigma). Semi-quantitative analysis was carried out using Quantity-one 1-D image analysis software version 4.6.5. A partition ratio with actin was calculated.

### **Statistical analysis**

Data are expressed as mean ± standard error of the mean (SEM). Statistical analysis was performed using either paired or unpaired Student's *t*-test or one-way ANOVA followed by Bonferroni test for selected pairs comparison. Values of  $p < 0.05$  were considered statistically significant;  $p < 0.01$  very significant; and  $p < 0.001$  extremely significant.



## RESULTS

### Validation of calpain cleavage sites

We recently provided compelling evidence that calpain-mediated proteolysis of mutant ataxin-3 generates C and N-terminal ~26 kDa fragments and a C-terminal ~34 kDa fragment based on antibody profiling with different monoclonal ataxin-3 antibodies (12, 13). According to the fragments molecular weights and a calpain algorithm (23), we predict they could be generated by calpain-mediated cleavage at ataxin-3 amino acids 194, 253 and 273. To elucidate the exact site of calpain cleavage, we designed calpain-resistant constructs ( $\Delta$  constructs), by deletion of five amino acids around the predicted calpain cleavage sites by inverse PCR mutagenesis, as the primary structure around the scissile bond is also important in the recognition process by calpains (23, 24). In addition, truncated forms of ataxin-3 considering the C-end of the aforementioned cleavage sites were designed as a positive control (Fig. 1A). First, to validate the calpain cleavage sites, we transfected the obtained constructs in HEK 293T (25). As predicted, truncation of wild-type ataxin-3 at amino acid 197 gave rise to the ~26 kDa fragment (27Q T197), while C-terminal truncated form of mutant ataxin-3 at amino acid 256 mimics the ~34 kDa fragment (72Q T256) and at amino acid 276 mimics the ~26 kDa fragment (72Q T276). We designed another construct, 72Q T285, that also gives rise to the ~26 kDa fragment, but without the nuclear localization signal (NLS, RKRR, aa. 282-285, (25, 26)) sequence to study the influence of proteolysis in the aggregates formation and subcellular localization of ataxin-3 with and without presence of the NLS sequence.

Calpain-resistant constructs ( $\Delta$  constructs) exhibited a similar molecular weight to the original forms of wild-type and mutant ataxin-3 (Fig. 1B).

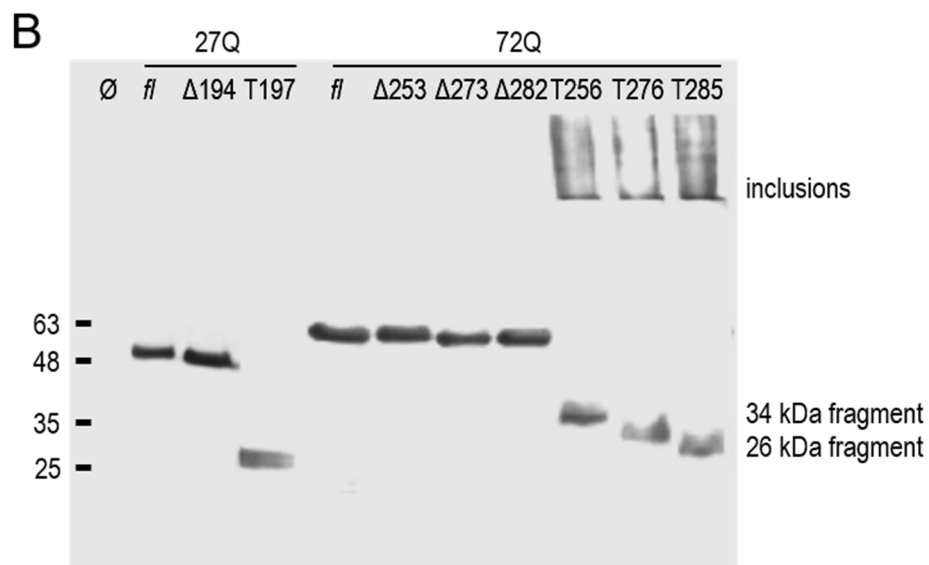
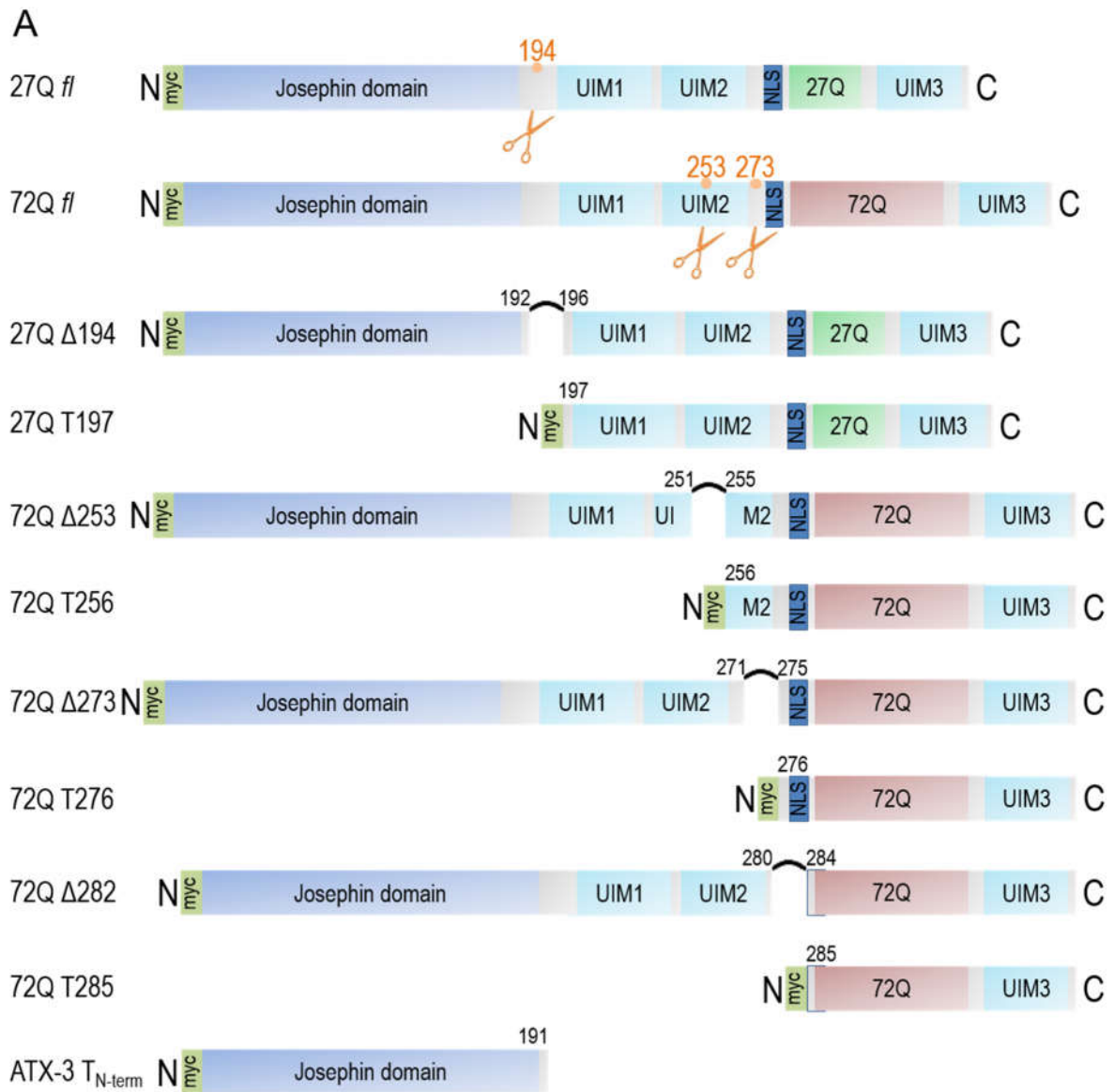


**Figure 1. Validation of calpain cleavage sites.** *A*, Schematic representation of full length (*fl*) wild-type ataxin-3 (27Q), mutant ataxin-3 (72Q) and the respective calpain cleavage sites identified. Calpain resistant constructs ( $\Delta$  construct) and their truncated forms (T construct) are also shown schematically. The amino acids deleted by mutagenesis and the truncated positions are shown above the constructs. The myc tag was attached to the N-terminus of each construct. *B*, Western-blot analysis of HEK 293T lysates transfected with truncated forms of ataxin-3 and calpain-resistant constructs. Ataxin-3 constructs were detected with an anti-myc antibody (clone 4A6), for a myc tag located at the N-terminal of each protein. Delta ( $\Delta$ ) means deletion of five amino acids around the calpain cleavage sites 194, 253, 273 and 282 of wild-type or mutant ataxin-3. C-terminal truncated form of ATX-3 27Q at amino acid 197 mimics the 26 kDa fragment (27Q T197), while C-terminal truncated form of ATX-3 72Q at amino acid 256 mimics the 34 kDa fragment (72Q T256) and at amino acid 276 mimics the 26 kDa fragment (72Q T276), which we have previously observed *in vivo* (Simões et al., 2012, 2014). 72Q T285 also mimics the formation of the 26 kDa fragment, but without the NLS sequence.  $\emptyset$  means non transfected and *fl* is full-length protein.

These validated constructs were then used to generate lentiviral vectors, which were transduced in the adult mouse brain to investigate which generated calpain cleavage fragment is more toxic and has a more drastic contribution to ataxin-3 nuclear localization, aggregation and neurotoxicity.

### **$\Delta$ constructs have a decreased cleavage and aggregation *in vivo***

For this purpose, lentiviral vectors encoding for truncated forms of ataxin-3 were injected in the left striatum hemisphere and calpain-resistant constructs in the right hemisphere. Five weeks after injection, mice were sacrificed and striatal tissue processed for western blot analysis.

Our results suggest that the mutation at amino acid 194 in wild-type ataxin-3 can significantly abrogate the production of the ~26 kDa fragment by 53% (Fig. 2).

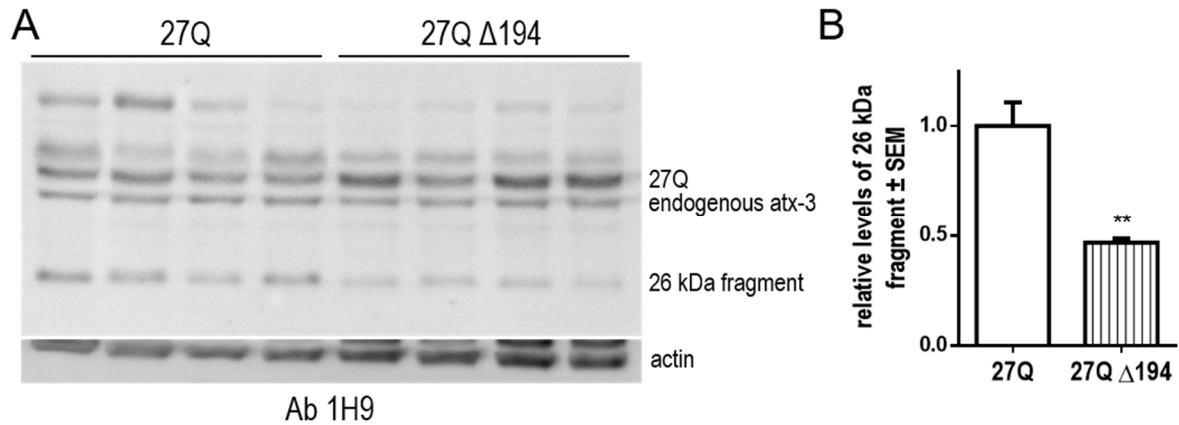


**Figure 2.** Wild-type ataxin-3  $\Delta$  construct has a decreased fragmentation *in vivo*. Western-blot analysis of mice 5 weeks post-injection of lentiviral vectors encoding for full-length wild-type ataxin-3 (27Q) and calpain-resistant construct with five amino acids deleted around the calpain cleavage site 194 (27Q  $\Delta$ 194). *A*, Membrane was incubated with ataxin-3 antibody (Ab 1H9). *B*, Densitometric quantification of 26 kDa fragment, using Ab 1H9, relative to actin (n=4, \*\*P<0.01).

Furthermore, as expected, deletion of five amino acids around amino acid 273 in mutant ataxin-3 decreased significantly the production of the ~26 kDa fragment by 57% (Fig. 3A,C). Surprisingly, the mutation at amino acid 253 in mutant ataxin-3 not only decreased significantly the production of the expected ~34 kDa fragment by 63% (Fig. 3A-B), but also the production of the ~26 kDa fragment by 62% (Fig. 3A,C), possibly due to alteration of higher order structural features, such as peptide bond access, backbone conformation, or three-dimensional structure, which are calpain cleavage characteristic features.

To investigate if this decreased fragmentation would be translatable to a reduction of the subsequent phenomena of aggregation, predicted by the “toxic fragment hypothesis”, we analysed the relative levels of C and N-terminal inclusions. Mutation at amino acid 253 in mutant ataxin-3 promoted a 31% significant decrease of C-terminal inclusions formation (Fig. 3A,D), being N-terminal inclusions not detected (Fig. 3E-F), while mutation at amino acid 273 conducted to a 26% and a 59% reduction of C and N-terminal inclusions formation, respectively (Fig. 3A,D-F).

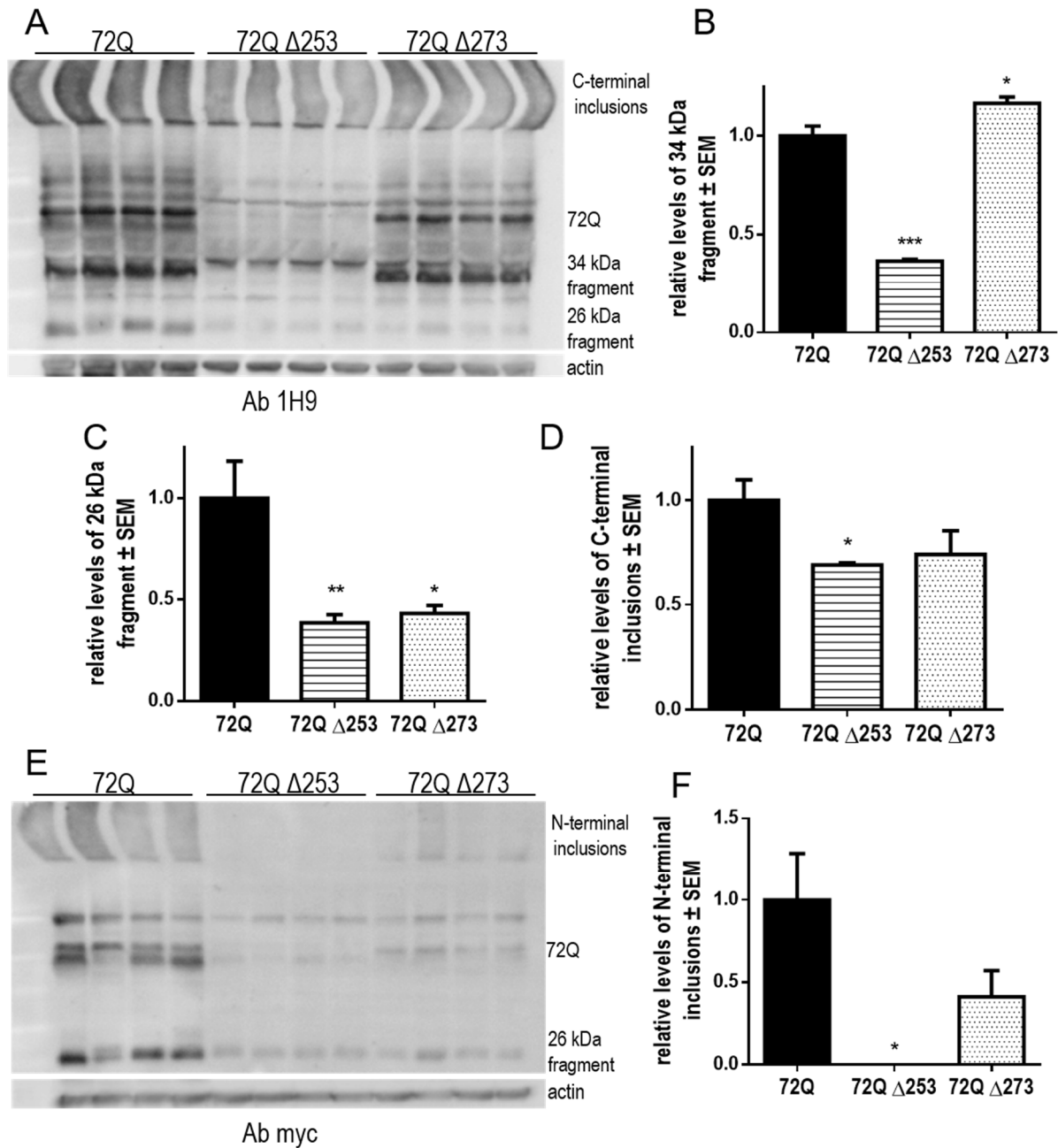


**Figure 3.** Mutant ataxin-3  $\Delta$  constructs have a decreased fragmentation and aggregation *in vivo*. Western-blot analysis of mice 5 weeks post-injection of lentiviral vectors encoding for full-length mutant ataxin-3 (72Q) and calpain-resistant constructs with five amino acids deleted around the calpain cleavage sites 253 (72Q  $\Delta$ 253) and 273 (72Q  $\Delta$ 273). *A*, Membrane was incubated with ataxin-3 antibody (Ab 1H9). *B-D*, Densitometric quantification of 34 kDa fragment, 26 kDa fragment and C-terminal inclusions levels, using Ab 1H9, relative to actin (n=4, \*P<0.05, \*\*P<0.01 and \*\*\*P<0.001). *E*, Membrane was incubated with myc tag antibody (Ab myc). *F*, Densitometric quantification of N-terminal inclusions levels, using Ab myc, relative to actin (n=4, \*P<0.05).

To monitor the subcellular localization of mutant ataxin-3, appearance of nuclear inclusions, loss of neuronal markers and cell death, we performed a new experiment using a similar paradigm but sacrificing the mice at a later time point (8 weeks post-injection) and processing the brains for immunohistochemistry. Similarly to what was observed by western-blot analysis 3 weeks before, mutation at amino acid 253 in mutant ataxin-3 continued to promote a 28% significant decrease of C-terminal inclusions formation (Fig. 4A-B,D-E,J), being N-terminal inclusions not detected (Fig. 4G-H,K), while mutation at amino acid 273 maintained a 7% and a 56% reduction of C and N-terminal inclusions formation, respectively (Fig. 4C,F,I-K).

These results support the idea that ataxin-3 cleavage by calpains is required for the subsequent aggregation process and that the simple mutation of calpain cleavage sites can reduce mutant ataxin-3 aggregation by suppressing the formation of ~26 kDa and ~34 kDa cleavage fragments.

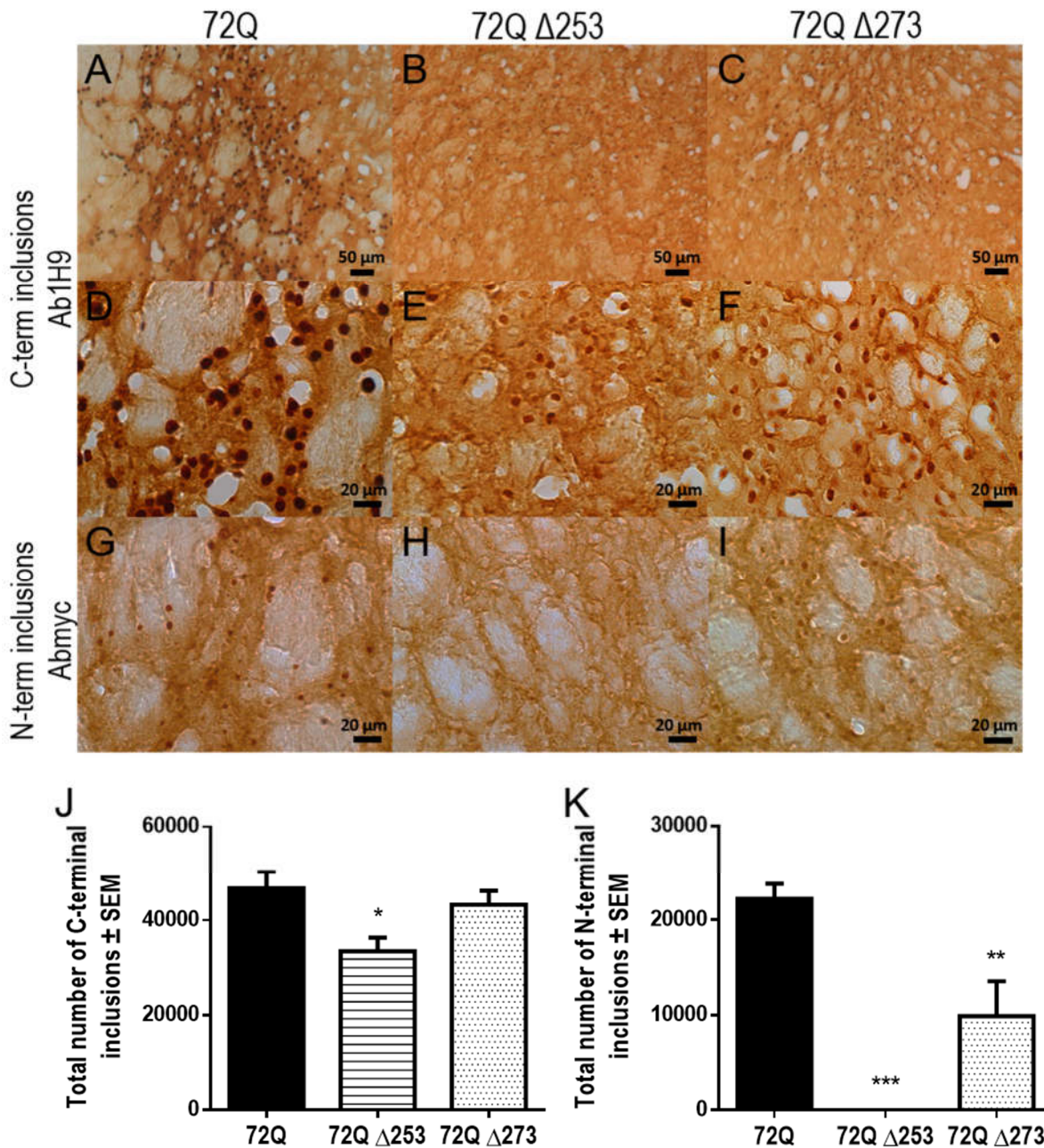


**Figure 4.**  $\Delta$  constructs continue to have a decreased aggregation *in vivo* at a later time point. Immunohistochemical analysis of mice 8 weeks post-injection of lentiviral vectors encoding for full-length mutant ataxin-3 (A, D, G; 72Q) and calpain-resistant constructs with five amino acids deleted around the calpain cleavage sites 253 (B, E, H; 72Q  $\Delta$ 253) and 273 (C, F, I; 72Q  $\Delta$ 273), using an (A-F) anti-ataxin-3 antibody (Ab1H9) or (G-I) anti-myc tag antibody (Ab myc). J, Quantification of the absolute number of ataxin-3 C-terminal inclusions; graph related to panel A-F. K, Quantification of the absolute number of ataxin-3 N-terminal inclusions; graph related to panel G-I. Values are expressed as mean  $\pm$  standard error of the mean (SEM) (n=7-9, \*P<0.05, \*\*P<0.01 and \*\*\*P<0.001).

### **Deletion of calpain cleavage sites restores cytoplasmic localization**

Since the nuclear localization is required for the *in vivo* manifestation of MJD neuropathology (16), we analysed the subcellular localization of the ataxin-3 species. In fact, the presence of intranuclear inclusions is considered a hallmark of MJD and other polyglutamine disorders (27), being ataxin-3 when non-expanded enriched in the cytoplasm, but upon polyglutamine expansion accumulated in the nucleus (4, 28-30).

As expected, full-length mutant ataxin-3 was assembled in large intranuclear inclusions and co-localized with ubiquitin (Fig. 5A-C,P). In addition, the expression of truncated forms of mutant ataxin-3 also led to the formation of intranuclear inclusions with co-localization of ataxin-3 and ubiquitin (Fig. 5D-I,P). On one hand, the decrease of the formation of the 26 kDa fragment by deletion of the respective calpain cleavage site, 72Q  $\Delta$ 273, restored significantly the cytoplasmic localization of ataxin-3 in 23% of cells, presenting a diffuse ubiquitin pattern, although the majority maintained the presence of intranuclear inclusions and co-localization with ubiquitin (Fig. 5M-P). On the other hand, deletion of five amino acids around amino acid 253, 72Q  $\Delta$ 253, which significantly decreased both fragments formation (Fig. 3B-C), re-established significantly ataxin-3 localization in the cytoplasm by 90%, and modifying the ubiquitin pattern from condensed to diffuse (Fig. 5J-L,P).

These results reinforce the importance of calpain-mediated proteolysis of mutant ataxin-3 for its translocation to the nucleus and consequent aggregation. Furthermore, these results suggest that an inhibition of both 34 and 26 kDa fragments formation is necessary to completely prevent nucleocytoplasmic shuttling activity of ataxin-3.



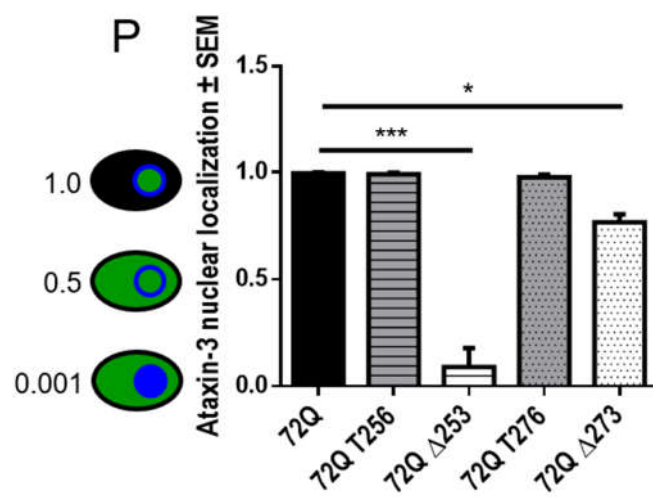
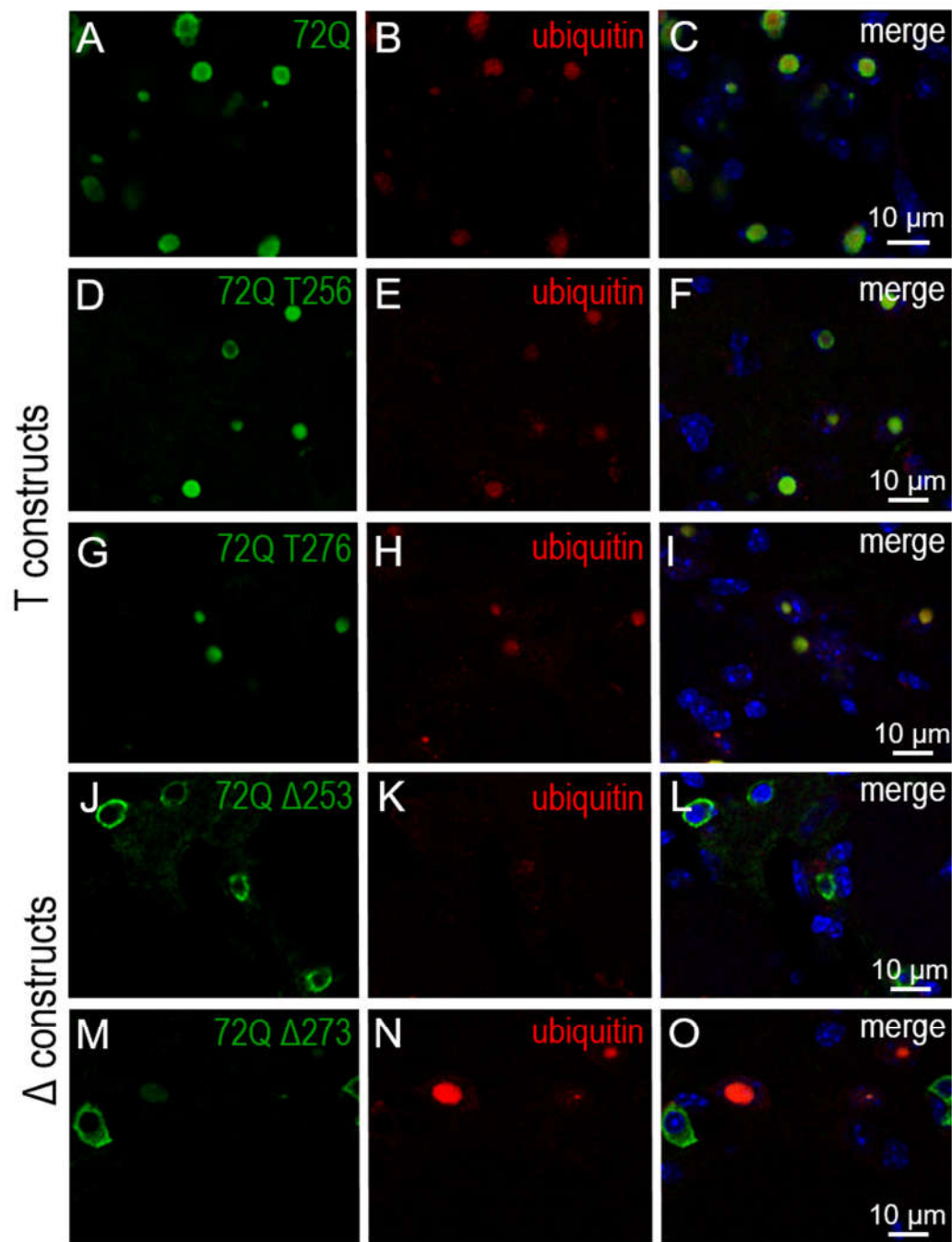


**Figure 5. Deletion of calpain cleavage sites restores cytoplasmic localization.** Immunohistochemical analysis of mice brains 8 weeks post-injection of lentiviral vectors encoding for (A-C), full-length mutant ataxin-3 (72Q), truncated ataxin-3 at position (D-F), 256 (72Q T256) and (G-I), 276 (72Q T276) and calpain-resistant constructs with five amino-acids deleted around the calpain cleavage sites (J-L), 253 (72Q  $\Delta$ 253) and (M-O), 273 (72Q  $\Delta$ 273). Coronal brain sections were stained for (A, D, G, J, M) myc tag located at the N-terminal of mutant ataxin-3 (Ab myc, green), (B, E, H, K, N) ubiquitin (Dako, red), nuclear marker (DAPI, blue). (C, F, I, L, O) merge images of the two respective previous letters. P, Quantification analysis of ataxin-3 nuclear localization, considering value 1 for nuclear localization, 0.5 for nuclear and cytoplasmic localization and 0.001 for cytoplasmic localization (n=3, \*P<0.05 and \*\*\*P<0.001).

### **The 26 kDa fragment is the major contributor to striatal degeneration**

To identify which fragment and corresponding sequence has the largest pathogenic effect and to evaluate the effects of the calpain-resistant constructs over neuronal dysfunction, we performed an immunohistochemical analysis for DARPP-32, a regulator of dopamine receptor signaling (31), as we have previously shown that it is down-regulated in the striatum of lentiviral and transgenic MJD animal models (20). The transduction of the ~26 kDa fragment (72Q T276; Fig. 6C,F) promoted a 33% significant increased loss of DARPP-32 immunoreactivity, when compared to the expression of the full-length form (72Q; Fig. 6A,F), while the transduction with the ~34 kDa fragment induced a similar loss of DARPP-32 staining (72Q T256; Fig. 6B,F), suggesting that it is the 26 kDa fragment, and not the 34 kDa fragment, that majorly contributes to striatal degeneration. Accordingly, even in the absence of NLS sequence, the transduction of 72Q T285 that also mimics the formation of the ~26 kDa fragment promotes a 21% significant increased loss of DARPP-32 immunoreactivity (data not shown), when compared to the expression of the full-length mutant ataxin-3, which is indicative of the

major toxic effect of the smaller fragment and of the minor contribution of the NLS once ataxin-3 is cleaved.

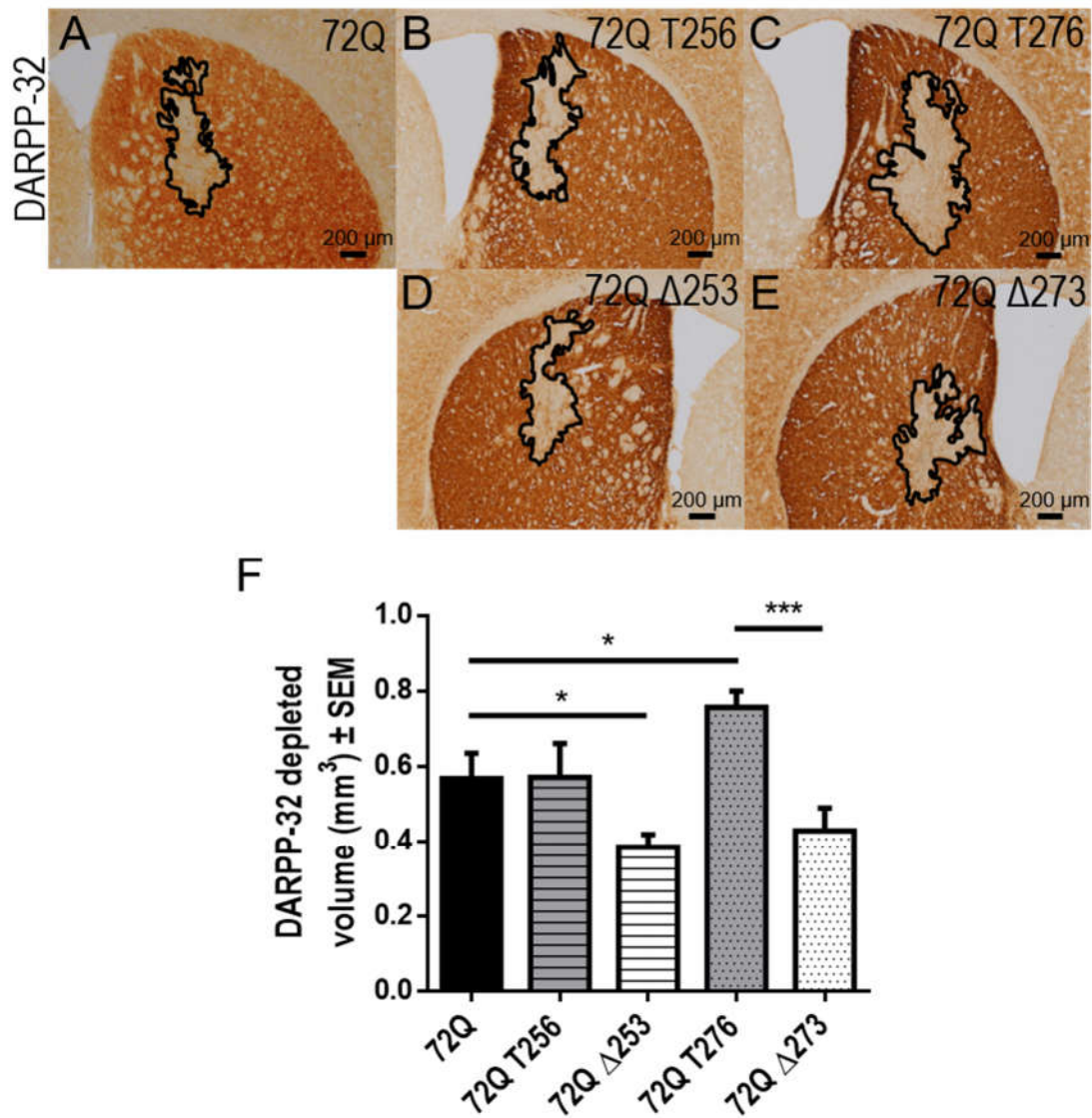


**Figure 6.** 26 kDa fragment induces an increased striatal degeneration while deletion of the calpain cleavage sites confers neuroprotection. Immunohistochemical analysis using an anti-DARPP-32 antibody (DAKO) of mice 8 weeks post-injection of lentiviral vectors encoding for *A*, full-length mutant ataxin-3 (72Q) and the C-terminal truncated forms of ATX-3 72Q at *B*, amino acid 256 (72Q T256, 34 kDa fragment) and *C*, 276 (72Q T276, 26 kDa fragment) and the respective resistant constructs, full length forms lacking *D*, five amino acids around 253 (72Q Δ253) and *E*, 273 (72Q Δ273). *F*, Quantification analysis of the DARPP-32 depleted volume in the mice brains (n=7-9, \*P<0.05 and \*\*\*P<0.001).

Previously, we have shown that calpain inhibition by either calpastatin overexpression or oral administration of a calpain inhibitor could promote neuroprotection decreasing significantly the volume of the region depleted of DARPP-32 immunoreactivity (12, 13). In this study, the sole deletion of one calpain cleavage site, *per se*, achieved a large neuroprotective effect. Actually, deletion of five amino acids around amino acid 253 (72Q  $\Delta$ 253, Fig. 7B,D) or 273 (72Q  $\Delta$ 273, Fig. 7C-D) led to a reduction by 25% and a significant reduction by 36%, respectively, of the loss of DARPP-32 staining, when compared to the full-length mutant ataxin-3, as soon as 5 weeks post-injection. At a later time point, 3 weeks after, the neuroprotective effect is still observed with a significant reduction of the volume of the region depleted of DARPP-32 immunoreactivity by 32% (72Q  $\Delta$ 253, Fig. 6D,F) and 25% (72Q  $\Delta$ 273, Fig. 6E-F) by deleting amino acids 251-255 and 271-275, respectively.

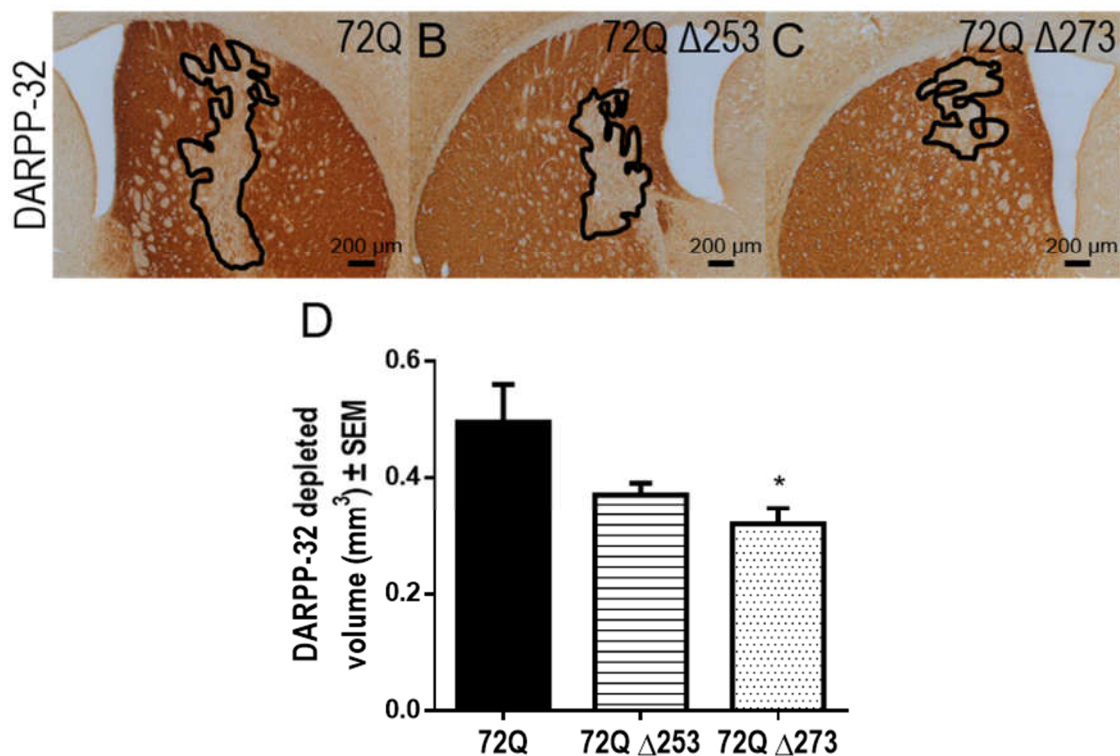


**Figure 7.** Deletion of the calpain cleavage site 273 and the respective 26 kDa fragment confers neuroprotection at an earlier time point. Immunohistochemical analysis using an anti-DARPP-32 antibody (DAKO) of mice 5 weeks post-injection of lentiviral vectors encoding for A, full-length mutant ataxin-3 (72Q) and the resistant constructs full length forms lacking B, five amino acids around 253

(72Q  $\Delta$ 253) and C, 273 (72Q  $\Delta$ 273). D, Quantification analysis of the DARPP-32 depleted volume in the mice brains (n=5-7, \*P<0.05).

Upon expression of the truncated form of wild-type ataxin-3 (27Q T197), it promoted an almost imperceptible loss of DARPP-32 immunoreactivity, being nevertheless the mutation at the calpain cleavage site 194 (27Q  $\Delta$ 194) able to significantly decrease the subtle loss (Fig. 8A-C,E). On the contrary to the C-terminal fragment of mutant ataxin-3, which promoted a prominent increase of DARPP-32 loss (Fig. 6B-C,F), the N-terminal fragment of ataxin-3 did not (ATX-3 T<sub>N-term</sub>), suggesting that its formation does not contribute to striatal degeneration (Fig. 8D-E).

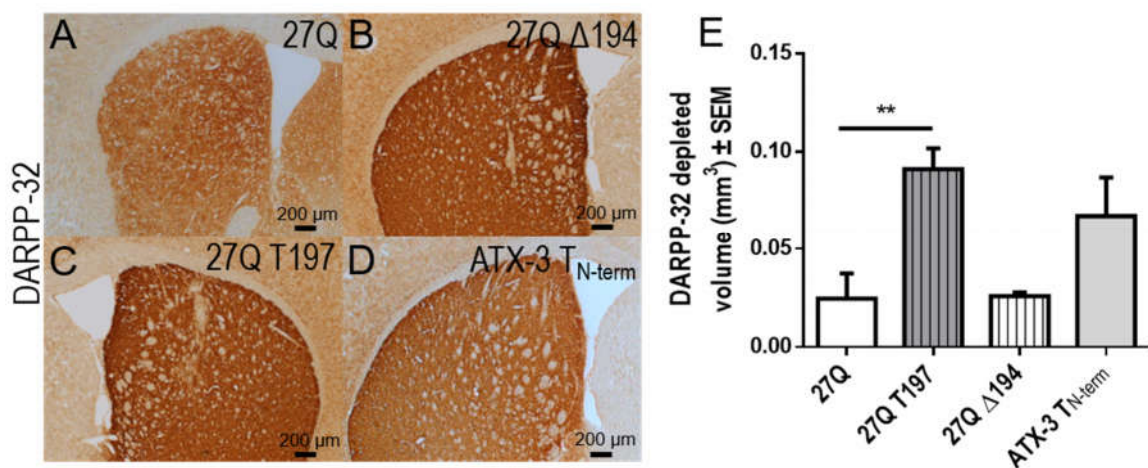


**Figure 8.** Truncated wild-type ataxin-3 induces an almost undetectable striatal degeneration, being the mutation at amino acid 194 able to decrease it. The ataxin-3 N-terminal fragment without polyQ stretch has a similar effect to wild-type constructs. Immunohistochemical analysis using an anti-DARPP-32 antibody (DAKO) of mice 8 weeks post-injection of lentiviral vectors encoding for A, full-length wild-type ataxin-3 (27Q), B, full length form of ATX-3 27Q calpain-resistant construct lacking five amino acids around amino acid 194 (27Q  $\Delta$ 194), C, the respective C-terminal truncated form of ATX-3 27Q at position 197 (27Q T197, 26 kDa fragment) and D, N-terminal truncated form of ataxin-3 at position 191 (ATX-3 T<sub>N-term</sub>). E, Quantification analysis of the DARPP-32 depleted volume in the mice brains (n=5-6, \*\*P<0.01 ).

Additionally, cresyl violet-stained sections further confirmed that both -34 kDa (72Q T256) and ~26 kDa (72Q T276) fragments formation, promoted an increased number of shrunken hyperchromatic nuclei by 23% and 29%, respectively (Fig. 9A-C,F; arrows), confirming that calpain-mediated proteolysis induces cell injury, in particular the smallest fragment. Deletion of five amino acids around the calpain cleavage sites revealed a marked reduction of the number of degenerated nuclei when compared to the expression of the truncated constructs, but not to the full-length form of ataxin-3 (Fig. 9D-F).

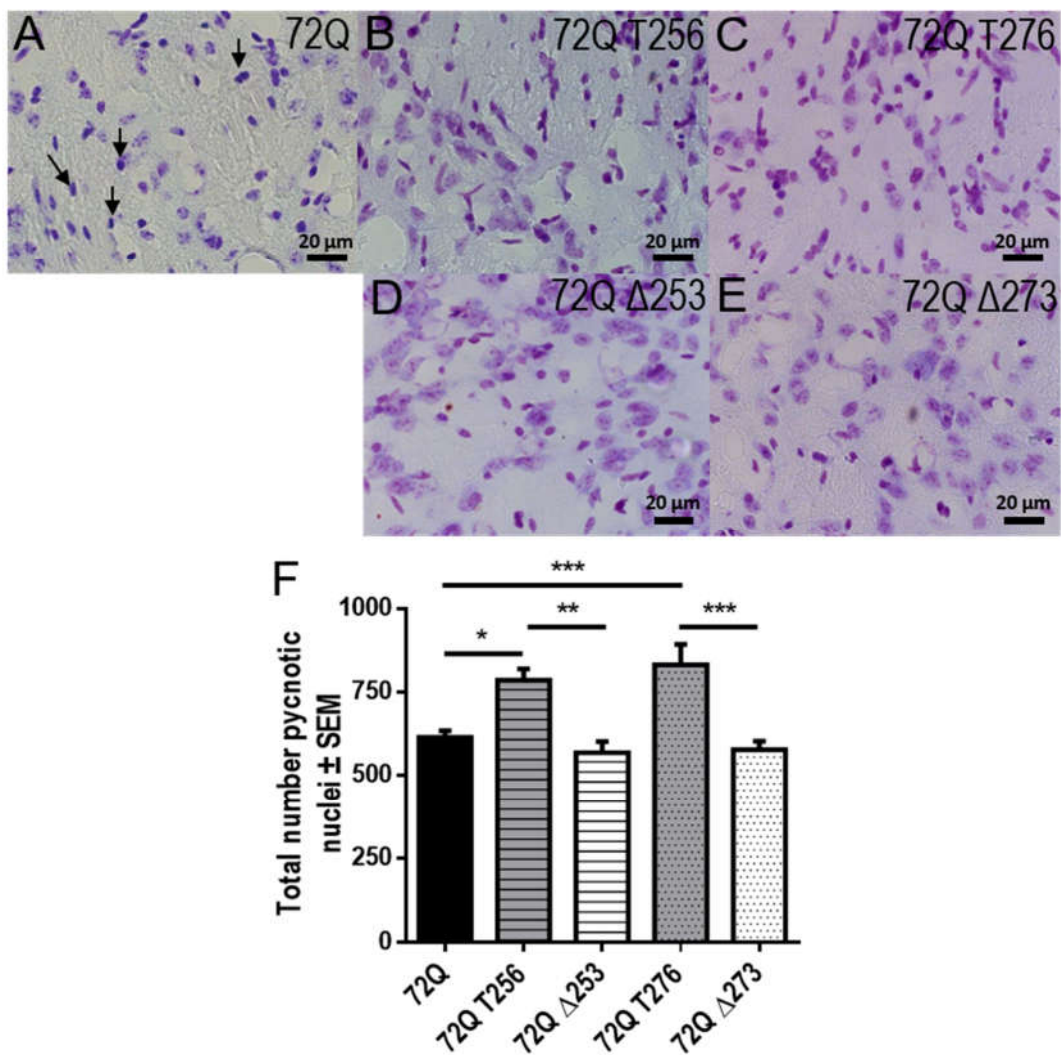


**Figure 9.** Mutant ataxin-3 truncated fragments promote an increased cell injury when compared to the full length protein. Cresyl violet staining of mice 8 weeks post-injection of lentiviral vectors encoding for A, full-length mutant ataxin-3 (72Q) and the C-terminal truncated forms of ATX-3 72Q at B, amino acid 256 (72Q T256, 34 kDa fragment) and C, 276 (72Q T276, 26 kDa fragment) and the respective

resistant constructs, full length forms lacking *D*, amino acids 251-255 (72Q  $\Delta$ 253) and *E*, 271-275 (72Q  $\Delta$ 273). *F*, Quantification analysis of the pycnotic nuclei (arrows) visible on cresyl violet-stained sections (n=7-9, \*P<0.05, \*\*P<0.01 and \*\*\*P<0.001).

Overall, these results are indicative that the C-terminal ~26 kDa fragment of mutant ataxin-3 has a major contribution to striatal degeneration and that the single deletion of one calpain cleavage site is able to promote a neuroprotective effect in a genetic mouse model of MJD.

### **Nuclear localization signal contributes initially to up to half of aggregation**

To evaluate the influence of the nuclear localization signal (NLS, RKRR, amino acid 282-285) (25, 26) in ataxin-3 aggregation, we designed a truncated form of ataxin-3 (72Q T285) that also mimics the formation of the ~26 kDa fragment, being the only difference relatively to 72Q T273 the absence of the conserved NLS sequence. The transduction of lentiviral vectors encoding for these truncated forms of ataxin-3 in the adult mouse brain revealed that even in the absence of the NLS sequence, C-terminal inclusions promoted by the expression of the ~26 kDa fragment can be formed (Fig. 10A). Nevertheless, aggregation occurs to a larger extent in the presence of the NLS by 43% (Fig. 10B), five weeks post-injection. At a later time point, 3 weeks after, this effect is lost, being the number of C-terminal inclusions formed similar (data not shown).

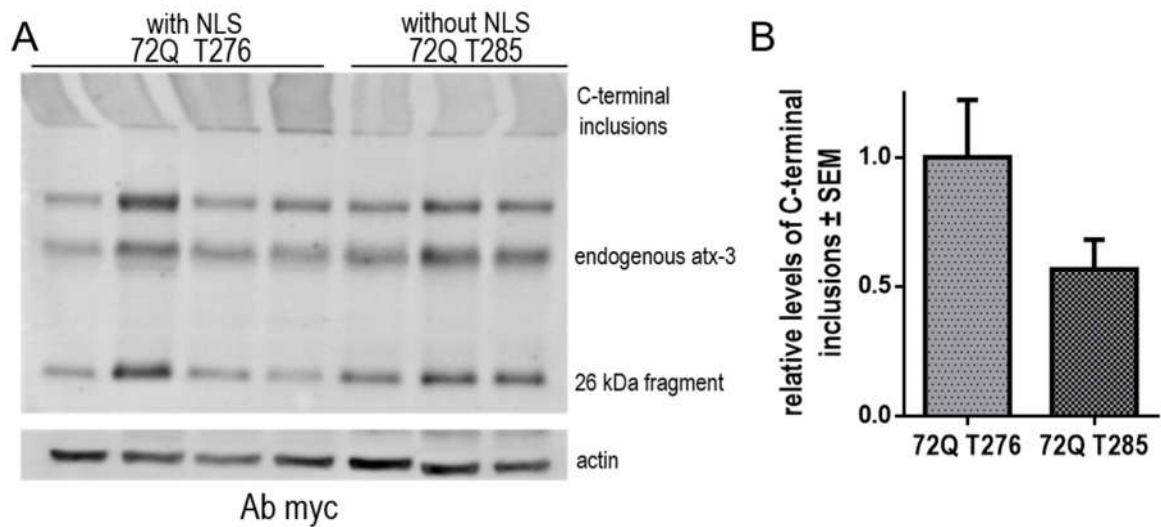


**Figure 10.** NLS contributes initially to up to half of aggregation. Western-blot analysis of mice 5 weeks post-injection of lentiviral vectors encoding for truncated forms of ataxin-3, using an anti-myc antibody (clone 4A6), for a myc tag located at the N-terminal of each truncated protein. C-terminal truncated forms of ATX-3 72Q at amino acid 276 and 285 mimic the 26 kDa fragment (72Q T276 and 72Q T285) with and without the nuclear localization signal, NLS (RKRR, amino acid 282-285), respectively. *B*, Densitometric quantification of C-terminal inclusions levels, using Ab myc, relative to actin (n=3-4).

Furthermore, the comparison between the deletion of five amino acids around the calpain cleavage site for -26 kDa fragment formation plus the NLS sequence (72Q  $\Delta$ 282) and the sole deletion of five amino acids around the calpain cleavage site for -26 kDa fragment formation (72Q  $\Delta$ 273) revealed that the number of C-terminal inclusions formation (Fig. 11A-B,E) and the volume of DARPP-32 loss (Fig. 11B-C,F) is also similar, which indicates that deletion of NLS does not promote an additional decrease in the formation of C-terminal inclusions, neither confers an additional neuroprotection.



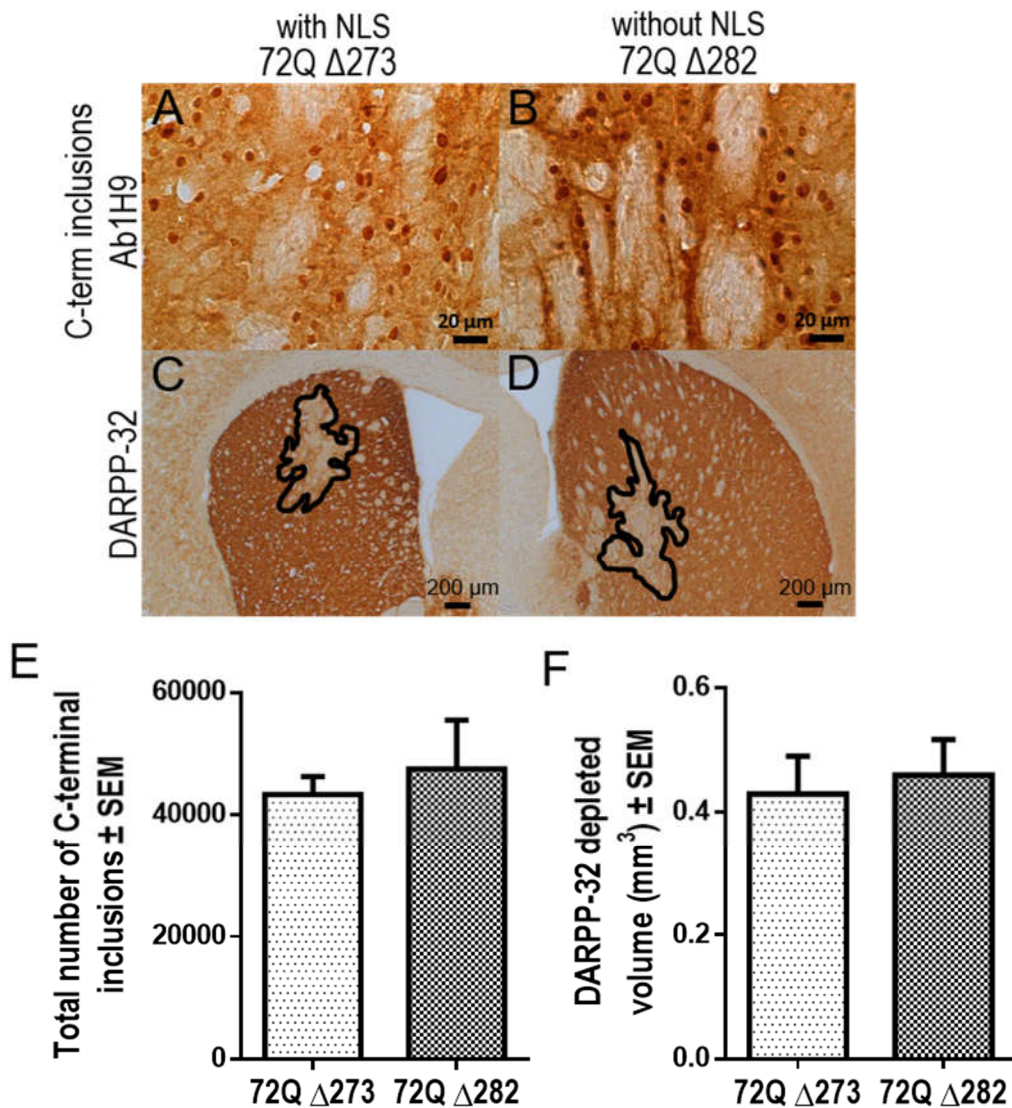


**Figure 11.** Deletion of NLS does not promote an additional decrease in the formation of C-terminal inclusions, neither confers an additional neuroprotection. Immunohistochemical analysis of mice 8 weeks post-injection of lentiviral vectors encoding for calpain-resistant constructs with five amino acids deleted around the calpain cleavage sites 273 (A, C; 72Q Δ273; with NLS) and 282 (B, D; 72Q Δ282; without NLS), using an (A-B) anti-ataxin-3 antibody (Ab1H9) or (C-D) anti-DARPP-32 antibody (DAKO). E, Quantification of the absolute number of ataxin-3 C-terminal inclusions; graph related to panel A-B. F, Quantification analysis of the DARPP-32 depleted volume in the mice brains; graph related to panel C-D. Values are expressed as mean ± standard error of the mean (SEM) (n=5-7).

These results suggest that although the NLS is not required for the seeding of intranuclear inclusions, it exacerbates their formation, indicating that it is only functional initially, while its deletion does not induce an additive neuroprotective effect, being the calpain cleavage site more important for pathology than the NLS.

## DISCUSSION AND CONCLUSIONS

In this work we provide *in vivo* evidence that calpains are the executioners of the proteolysis of mutant ataxin-3, required for a) the formation of the 34 and 26 kDa fragments, b) their translocation to the nucleus and c) aggregation. We have further identified the calpain cleavage sites *in vivo*. Although our studies demonstrate that it is the 26 kDa fragment the major contributor to striatal degeneration, it is necessary to decrease both fragments formation to completely prevent intranuclear localization of ataxin-3, which is achieved by simply deleting the calpain cleavage site at amino acids 251-255. The use of calpain-resistant constructs as a genetic model of calpain inhibition further confirmed a neuroprotective effect, consequent to a decreased proteolysis and nuclear aggregation.

The neurotoxicity associated with MJD has been proposed to be derived from proteolytic cleavage of the mutant ataxin-3, an idea referred to as the toxic fragment hypothesis (5). Furthermore, the proteolytic event was reported to be the trigger of the aggregation process (3), being either caspases (6-8) or calpains (9, 10, 12-14) the proteases involved in this process. Based on work with *in vitro* models, mutant ataxin-3 has been proposed to be cleaved by calpains at amino acid 257 (3); 60, 200, 260 (9) and more recently 208 and 256 (14), having this latter study been published while we were finalizing this work. The two studies are concordant on providing compelling evidence of the involvement of calpains and their cleavage sites, at least approximately, in Machado-Joseph disease. Nevertheless, our work brings new insights as it was performed *in vivo*, without external protease activation, and we further analyzed the differential cleavage between wild-type and mutant ataxin-3, which fragment is more toxic and whether the mutagenesis of the amino acids would not only promote a decrease in fragmentation, the previously addressed step, but also aggregation and promotion of neuroprotection.

Accordingly, in this study, we investigated the exact site of calpain-mediated proteolysis *in vivo*, by conjugation of the previous identified calpain-mediated mutant ataxin-3 cleavage fragments molecular weights: 26 and 34 kDa (12, 13) and a calpain algorithm (23) (Fig. 1A). Our results confirm that the truncation of ataxin-3 at calpain-cleavage sites gives rise to the fragments at the expected molecular weights (Fig. 1B) and that their mutation leads to a decrease of their formation (Fig. 2, 3A-C). In this sense, these results confirm calpains as the proteases responsible for the proteolytic event. Cleavage of wild-type ataxin-3 at amino acid 197 leads to the formation of a 26 kDa fragment (Fig. 2), while cleavage of mutant ataxin-3 at amino acids 256 and 276 generates the 34 and 26 kDa fragments, respectively (Fig. 3A-C). Nevertheless, the total abrogation of the cleavage fragments formation was not observed with the constructs generated by inverse PCR mutagenesis, possibly because the cleavage specificity of calpains is only weakly dictated by the primary sequence of its protein substrates (23, 24), being possible that calpains may still continue to cleave the protein right next to the mutated site. The cleavage within amino acids 251-255 originates a C-terminal fragment at amino acid 256, recently identified by the mass spectrometry study of Weber and collaborators. Similarly, cleavage within 271-275 gives rise to the tested C-terminal fragment at amino acid 276, next to amino acid 277 also identified by Weber et al. by calpain overlay assay, being both, two sites of the four, major cleavage sites identified *in vitro* at positions H187, D208, S256 and T277 (14). The amino acid 197 is also close to the positions 187 and 208, although our study suggests that it is important for calpain-mediated proteolysis of wild-type ataxin-3, but not for mutant ataxin-3, whose cleavage would not lead to the formation of the 26 and 34 kDa mutant fragments identified *in vivo*. Nonetheless, the slight differences might be due to the expression of ataxin-3 with different number of CAG repeats. While in our study, ataxin-3 has either 27 or 72 CAG repeats for wild-type and mutant ataxin-3, respectively, in Weber and collaborators study, it varies from 15-22 and 62-148 CAG repeats depending on the experiments.

Furthermore, the addition of the myc tag at the N-terminal of ataxin-3 in our study may also hinder a different kinetics of cleavage.

Upon polyglutamine expansion, ataxin-3 accumulates in the nucleus as intranuclear inclusions, which are a hallmark of the pathology (27, 29, 32). As expected, the truncated ataxin-3 mimicking both fragments formation led to the formation of intranuclear inclusions with co-localization of ataxin-3 with ubiquitin (Fig. 5D-I,P), possibly by passing the nuclear pore through passive diffusion. The expression of these truncated fragments bearing 72Q within the nucleus as intranuclear inclusions was previously demonstrated by our group in HEK 293T cells (33), and now confirmed *in vivo*, on the contrary to Weber et al. study, in which C-terminal fragments with 148Q exhibited mainly cytoplasmic localization, also in HEK 293T cells (14), which strengthens the importance of the number of CAG repeats and the choice of the closest physiologic related model to MJD patients to draw conclusions. Importantly, the mutation of the calpain cleavage sites was able to mediate a reduction of the intranuclear inclusions formation (Fig. 3A,D-F, 4). In fact, by using inverse PCR mutagenesis to develop a calpain-resistant model of MJD, we were able to confirm the importance of calpain-mediated proteolysis for the translocation of ataxin-3 to the nucleus and the aggregation process.

Actually, this nuclear localization is further required for the *in vivo* manifestation of MJD neuropathology. Accordingly, transgenic mice with 148 CAGs but attached to a nuclear export signal only develop a milder phenotype with few inclusions (16). In addition, our results suggest that although the single decrease of the formation of the 26 kDa fragment is able to partially prevent the translocation of ataxin-3 to the nucleus, it is only when both the 34 and the 26 kDa fragments are significantly decreased that a fully reconditioning of ataxin-3 to the cytoplasm is possible (Fig. 5J-P). Overall, this work clarifies ataxin-3 nucleocytoplasmic shuttling activity, which has also been shown to be promoted by a) recognition of specific nuclear localization signals (NLS) or nuclear export signals (NES) (17, 25, 26, 34, 35), b)

phosphorylation on serine residues within ataxin-3 (18, 36) and c) proteotoxic stress, such as heat shock and oxidative stress (19).

Furthermore, this work also elucidates the importance of the NLS sequence in the nuclear transport of ataxin-3. In fact, although a putative NLS was identified upstream to the polyQ sequence (RKRR, aminoacid 282-285) (26), being highly conserved among species, no functional consensus was attributed to this signal (17, 25, 34). Our results suggest that even in the absence of the NLS sequence, intranuclear inclusions formation (Fig. 10, 11A-B,E) and striatal degeneration (Fig. 11C-D,F) can occur. Nevertheless, NLS presence exacerbates these mechanisms at an earlier time point, which is indicative that although it is not an absolute requisite for the initial seeding process, started by calpain-mediated proteolysis, which generates cleavage fragments followed by ataxin-3 translocation to the nucleus, it is functional initially. In addition, despite previous evidences suggesting that the non-polyglutamine containing ataxin-3 N-terminus fragment is also toxic (37), our results reinforce the importance of the C-terminal fragment cytotoxicity (4, 5). In fact, neither wild-type ataxin-3 C-terminal fragment nor ataxin-3 N-terminal fragment promoted a significant DARPP-32 depleted volume (Fig. 8) regardless of their formation upon calpain-mediated proteolysis, suggesting that these fragments may not be cytotoxic and questioning their contribution for MJD pathology *per se*.

Altogether, these results support the toxic fragment hypothesis, considering the fragment bearing the polyglutamine extended stretch. Although it is the 26 kDa fragment the major contributor to striatal degeneration (Fig. 6) and cell injury (Fig. 9), decrease of both the ~26 kDa and the ~34 kDa fragments is necessary for cytoplasmic localization (Fig. 5) and for neuroprotection at a later time point (Fig. 6). This latter fact is suggested by a bigger decrease of DARPP-32 volume loss of 72Q  $\Delta$ 253, when compared to 72Q  $\Delta$ 273, which means that a higher neuroprotection is possible upon the decrease of the formation of the 34 and 26 kDa fragments, when compared to the single decrease of the 26 kDa fragment (Fig. 6), whose

neuroprotective effect is better observed at an earlier time point (Fig. 7). Overall, our previous knowledge using adeno-associated viral vectors encoding for calpastatin or administration of synthetic calpain inhibitors together with these results suggest that the genetic manipulation of calpain cleavage sites is also beneficial as a therapeutic approach. This means that not only one can consider this genetic model as a proof-of-principle of the involvement of calpain-mediated proteolysis as a pathogenic mechanism of MJD, but also that the identification of the calpain cleavage sites will allow the design of more specific drugs or the use of tools for genome editing at a specific location.

In conclusion, this study identifies the calpain cleavage sites for the first time in a mouse model: amino acid 194 for the wild-type ataxin-3, and amino acids 253 and 273 for the mutant ataxin-3 (Fig. 1A), along with the adjacent positions to the scissile bond, also determinant for the calpain recognition and optimal cleavage. The mutation of these sites implicates calpains in ataxin-3 translocation to the nucleus, an involvement dependent of the production of both the ~34 and the ~26 kDa fragments. Nevertheless, it is the smaller fragment the major contributor for striatal degeneration, independently of the NLS sequence. Furthermore, the genetic deletion of these sites prevents neuronal dysfunction and neurodegeneration, suggesting a neuroprotective effect. Therefore, these findings reinforce that calpain-mediated proteolysis is a promising target for MJD therapeutic intervention.

*Conflict of interest statement:* The authors declare no conflict of interest.

## **ACKNOWLEDGEMENTS**

The authors wish to thank Luísa Cortes and Margarida Caldeira from the CNC – MICC Imaging facility for image acquisition assistance on confocal microscopy.

## **FUNDING**

This work was funded by the ERDF through the Regional Operational Program Center 2020, Competitiveness Factors Operational Program (COMPETE 2020) and National Funds through FCT (Foundation for Science and Technology) - BrainHealth2020 projects (CENTRO-01-0145-FEDER-000008), ViraVector (CENTRO-01-0145-FEDER-022095), CortaCAGs (POCI-01-0145-FEDER-016719) and POCI-01-0145-FEDER-007440, as well as SFRH/BPD/87341/2012, SFRH/BD/87048/2012, SFRH/BD/74993/2010 and SFRH/BD/87404/2012 to ATS, VC, JDN and JCS, respectively (FCT), and AFM-Telethon and the SynSpread, ESMI and ModelPolyQ under the EU Joint Program - Neurodegenerative Disease Research (JPND), the last two co-funded by the European Union H2020 program, GA No.643417; by National Ataxia Foundation (USA), the American Portuguese Biomedical Research Fund (APBRF) and the Richard Chin and Lily Lock Machado-Joseph Disease Research Fund.

## REFERENCES

1. Ranum LP, Lundgren JK, Schut LJ, Ahrens MJ, Perlman S, Aita J, et al. Spinocerebellar ataxia type 1 and Machado-Joseph disease: incidence of CAG expansions among adult-onset ataxia patients from 311 families with dominant, recessive, or sporadic ataxia. *Am J Hum Genet.* 1995 Sep;57(3):603-8.
2. Kawaguchi Y, Okamoto T, Taniwaki M, Aizawa M, Inoue M, Katayama S, et al. CAG expansions in a novel gene for Machado-Joseph disease at chromosome 14q32.1. *Nat Genet.* 1994 Nov;8(3):221-8.
3. Haacke A, Broadley SA, Boteva R, Tzvetkov N, Hartl FU, Breuer P. Proteolytic cleavage of polyglutamine-expanded ataxin-3 is critical for aggregation and sequestration of non-expanded ataxin-3. *Hum Mol Genet.* 2006 Feb 15;15(4):555-68.
4. Goti D, Katzen SM, Mez J, Kurtis N, Kiluk J, Ben-Haiem L, et al. A mutant ataxin-3 putative-cleavage fragment in brains of Machado-Joseph disease patients and transgenic mice is cytotoxic above a critical concentration. *J Neurosci.* 2004 Nov 10;24(45):10266-79.
5. Ikeda H, Yamaguchi M, Sugai S, Aze Y, Narumiya S, Kakizuka A. Expanded polyglutamine in the Machado-Joseph disease protein induces cell death in vitro and in vivo. *Nat Genet.* 1996 Jun;13(2):196-202.
6. Berke SJ, Schmied FA, Brunt ER, Ellerby LM, Paulson HL. Caspase-mediated proteolysis of the polyglutamine disease protein ataxin-3. *J Neurochem.* 2004 May;89(4):908-18.
7. Wellington CL, Ellerby LM, Hackam AS, Margolis RL, Trifiro MA, Singaraja R, et al. Caspase cleavage of gene products associated with triplet expansion disorders generates truncated fragments containing the polyglutamine tract. *J Biol Chem.* 1998 Apr 10;273(15):9158-67.
8. Jung J, Xu K, Lessing D, Bonini NM. Preventing Ataxin-3 protein cleavage mitigates degeneration in a *Drosophila* model of SCA3. *Hum Mol Genet.* 2009 Dec 15;18(24):4843-52.
9. Haacke A, Hartl FU, Breuer P. Calpain inhibition is sufficient to suppress aggregation of polyglutamine-expanded ataxin-3. *J Biol Chem.* 2007 Jun 29;282(26):18851-6.
10. Hubener J, Weber JJ, Richter C, Honold L, Weiss A, Murad F, et al. Calpain-mediated ataxin-3 cleavage in the molecular pathogenesis of spinocerebellar ataxia type 3 (SCA3). *Hum Mol Genet.* 2013 Feb 1;22(3):508-18.



11. Koch P, Breuer P, Peitz M, Jungverdorben J, Kesavan J, Poppe D, et al. Excitation-induced ataxin-3 aggregation in neurons from patients with Machado-Joseph disease. *Nature*. 2011 Dec 22;480(7378):543-6.
12. Simões AT, Gonçalves N, Koeppen A, Déglon N, Kügler S, Duarte CB, et al. Calpastatin-mediated inhibition of calpains in the mouse brain prevents mutant ataxin 3 proteolysis, nuclear localization and aggregation, relieving Machado-Joseph disease. *Brain*. 2012 Aug;135(Pt 8):2428-39.
13. Simoes AT, Goncalves N, Nobre RJ, Duarte CB, Pereira de Almeida L. Calpain inhibition reduces ataxin-3 cleavage alleviating neuropathology and motor impairments in mouse models of Machado-Joseph disease. *Hum Mol Genet*. 2014 Sep 15;23(18):4932-44.
14. Weber JJ, Golla M, Guaitoli G, Wanichawan P, Hayer SN, Hauser S, et al. A combinatorial approach to identify calpain cleavage sites in the Machado-Joseph disease protein ataxin-3. *Brain*. 2017 May 1;140(5):1280-99.
15. Yang W, Dunlap JR, Andrews RB, Wetzel R. Aggregated polyglutamine peptides delivered to nuclei are toxic to mammalian cells. *Hum Mol Genet*. 2002 Nov 1;11(23):2905-17.
16. Bichelmeier U, Schmidt T, Hubener J, Boy J, Ruttiger L, Habig K, et al. Nuclear localization of ataxin-3 is required for the manifestation of symptoms in SCA3: in vivo evidence. *J Neurosci*. 2007 Jul 11;27(28):7418-28.
17. Antony PM, Mantele S, Mollenkopf P, Boy J, Kehlenbach RH, Riess O, et al. Identification and functional dissection of localization signals within ataxin-3. *Neurobiol Dis*. 2009 Nov;36(2):280-92.
18. Mueller T, Breuer P, Schmitt I, Walter J, Evert BO, Wullner U. CK2-dependent phosphorylation determines cellular localization and stability of ataxin-3. *Hum Mol Genet*. 2009 Sep 1;18(17):3334-43.
19. Reina CP, Zhong X, Pittman RN. Proteotoxic stress increases nuclear localization of ataxin-3. *Hum Mol Genet*. 2010 Jan 15;19(2):235-49.
20. Alves S, Regulier E, Nascimento-Ferreira I, Hassig R, Dufour N, Koeppen A, et al. Striatal and nigral pathology in a lentiviral rat model of Machado-Joseph disease. *Hum Mol Genet*. 2008 Jul 15;17(14):2071-83.
21. de Almeida LP, Zala D, Aebischer P, Déglon N. Neuroprotective effect of a CNTF-expressing lentiviral vector in the quinolinic acid rat model of Huntington's disease. *Neurobiol Dis*. 2001 Jun;8(3):433-46.

22. Barde I, Salmon P, Trono D. Production and titration of lentiviral vectors. *Curr Protoc Neurosci.* 2010 Oct;Chapter 4:Unit 4 21.
23. Tompa P, Buzder-Lantos P, Tantos A, Farkas A, Szilagyí A, Banoczi Z, et al. On the sequential determinants of calpain cleavage. *J Biol Chem.* 2004 May 14;279(20):20775-85.
24. Cuerrier D, Moldoveanu T, Davies PL. Determination of peptide substrate specificity for mu-calpain by a peptide library-based approach: the importance of primed side interactions. *J Biol Chem.* 2005 Dec 9;280(49):40632-41.
25. Albrecht M, Golatta M, Wullner U, Lengauer T. Structural and functional analysis of ataxin-2 and ataxin-3. *Eur J Biochem.* 2004 Aug;271(15):3155-70.
26. Tait D, Riccio M, Sittler A, Scherzinger E, Santi S, Ognibene A, et al. Ataxin-3 is transported into the nucleus and associates with the nuclear matrix. *Hum Mol Genet.* 1998 Jun;7(6):991-7.
27. Paulson HL, Perez MK, Trottier Y, Trojanowski JQ, Subramony SH, Das SS, et al. Intranuclear inclusions of expanded polyglutamine protein in spinocerebellar ataxia type 3. *Neuron.* 1997 Aug;19(2):333-44.
28. Paulson HL, Das SS, Crino PB, Perez MK, Patel SC, Gotsdiner D, et al. Machado-Joseph disease gene product is a cytoplasmic protein widely expressed in brain. *Ann Neurol.* 1997 Apr;41(4):453-62.
29. Schmidt T, Landwehrmeyer GB, Schmitt I, Trottier Y, Auburger G, Laccone F, et al. An isoform of ataxin-3 accumulates in the nucleus of neuronal cells in affected brain regions of SCA3 patients. *Brain Pathol.* 1998 Oct;8(4):669-79.
30. Cemal CK, Carroll CJ, Lawrence L, Lowrie MB, Ruddle P, Al-Mahdawi S, et al. YAC transgenic mice carrying pathological alleles of the MJD1 locus exhibit a mild and slowly progressive cerebellar deficit. *Hum Mol Genet.* 2002 May 1;11(9):1075-94.
31. Greengard P, Allen PB, Nairn AC. Beyond the dopamine receptor: the DARPP-32/protein phosphatase-1 cascade. *Neuron.* 1999 Jul;23(3):435-47.
32. Yamada M, Hayashi S, Tsuji S, Takahashi H. Involvement of the cerebral cortex and autonomic ganglia in Machado-Joseph disease. *Acta Neuropathol.* 2001 Feb;101(2):140-4.
33. Carmona V, Cunha-Santos J, Onofre I, Simoes AT, Vijayakumar U, Davidson BL, et al. Unravelling Endogenous MicroRNA System Dysfunction as a New Pathophysiological Mechanism in Machado-Joseph Disease. *Mol Ther.* 2017 Apr 5;25(4):1038-55.
34. Macedo-Ribeiro S, Cortes L, Maciel P, Carvalho AL. Nucleocytoplasmic shuttling activity of ataxin-3. *PLoS One.* 2009;4(6):e5834.

35. Rodrigues AJ, Coppola G, Santos C, Costa Mdo C, Ailion M, Sequeiros J, et al. Functional genomics and biochemical characterization of the *C. elegans* orthologue of the Machado-Joseph disease protein ataxin-3. *FASEB J.* 2007 Apr;21(4):1126-36.
36. Pastori V, Sangalli E, Coccetti P, Pozzi C, Nonnis S, Tedeschi G, et al. CK2 and GSK3 phosphorylation on S29 controls wild-type ATXN3 nuclear uptake. *Biochim Biophys Acta.* 2010 Jul-Aug;1802(7-8):583-92.
37. Hubener J, Vauti F, Funke C, Wolburg H, Ye Y, Schmidt T, et al. N-terminal ataxin-3 causes neurological symptoms with inclusions, endoplasmic reticulum stress and ribosomal dislocation. *Brain.* 2011 Jul;134(Pt 7):1925-42.